PERGAMON

International Journal of Solids and Structures 39 (2002) 1591–1619

INTERNATIONAL JOURNAL OF SOLIDS and STRUCTURES

www.elsevier.com/locate/ijsolstr

Exact solution for mixed boundary value problems at anisotropic piezoelectric bimaterial interface and unification of various interface defects

Xu Wang, Ya-peng Shen *

Department of Engineering Mechanics, Xi'an Jiaotong University, Xi'an, Shaanxi Province 710049, China

Received 11 November 2000; received in revised form 17 September 2001

Abstract

The special mixed boundary value problem in which a debonded conducting rigid line inclusion is embedded at the interface of two piezoelectric half planes is solved analytically by employing the 8-D Stroh formalism. Different from existing interface insulating crack model and interface conducting rigid line inclusion model, the presently analyzed model is based on the assumption that all of the physical quantities, i.e., tractions, displacements, normal component of electric displacements and electric potential, are discontinuous across the interface defect. Explicit solutions for stress singularities at the tips of debonded conducting rigid line inclusion are obtained. Closed form solutions for the distribution of tractions on the interface, surface opening displacements and jump in electric potential on the debonded inclusion are also obtained, in addition real form solutions for these physical quantities are derived. Various forms of interface defect problems encountered in practice are solved within a unified framework and the stress singularities induced by those interface defects are discussed in detail. Particularly, we find that the analysis of interface cracks between the embedded electrode layer and piezoelectric ceramics can also be carried out within the unified framework. © 2002 Published by Elsevier Science Ltd.

Keywords: Piezoelectricity; Mixed boundary value problem; Standard Stroh formalism and its modifications; Explicit solution; Stress singularity

1. Introduction

The mixed boundary value problems in isotropic and anisotropic elasticity have received many investigators' attention. Keer (1975) considered the problem of a debonded rigid thin circular disk in a single isotropic material. Through integral transform, he finally reduced the problem to two decoupled Riemann–Hilbert problems and obtained closed form expressions for the axial stiffness of the system. Gladwell (1999) treated the problems of bonded or partially bonded contact of a rigid circular disk between dissimilar isotropic half spaces. Through systematic application of Fourier and Abel transforms, he reduced the problem to the solution to Riemann–Hilbert problems and also obtained closed form expressions for the axial stiffness

* Corresponding author. Fax: +86-29-323-7910.
E-mail address: ypshen@xjtu.edu.cn (Y.-p. Shen).

0020-7683/02/$ - see front matter © 2002 Published by Elsevier Science Ltd.
PII: S0020-7683(01)00273-6

of the composite system. Muskhelishvili (1953) addressed the straight cut problem in a homogeneous isotropic material. Tractions are prescribed on one side of the cut while displacements are prescribed on the other side of the cut. Markenscoff and Ni (1996) investigated the problem of a debonded rigid line inclusion at the interface of two dissimilar isotropic half planes. Their method of solution is based on distributing densities of both dislocations and line loads on the cut surface, and they reduced the original problem to coupled singular integral equations, which were then solved analytically through diagonalization. In their discussions, they obtained the explicit relationship between stress singularities and the material constants combination. Ting (1986) studied the stress singularities for crack, inclusion and mixed boundary value problems at the interface of dissimilar anisotropic (including isotropic) bimaterials by employing the Stroh formalism (6-D). For crack and inclusion problems, he obtained explicit solutions for the stress singularities; while for the mixed boundary value problems, he only presented the explicit solutions for isotropic bimaterials. He also proved that stress singularities for all the three cases are invariant with respect to the orientation of the interface relative to the bimaterials. Also by employing the Stroh formalism (6-D), Homulka and Keer (1995) solved the problem of debonded rigid line inclusion at the interface of dissimilar anisotropic bimaterials. They reduced the mixed boundary value problem to coupled Riemann–Hilbert problems and decoupled them to single Hilbert problem through adopting a clever decoupling method proposed by Clements (1971). In their analyses, the rigid line inclusion which was termed anchor in their paper, may experience a rotation about the x_3-axis and the angle of rotation is determined through balance of moment on the inclusion.

Piezoelectric problems of cracks and inclusions under mechanical and electrical loads continue to attract attention of the researchers because of their numerous practical applications. Recent contributions include the works of Kuo and Barnett (1991), Suo et al. (1992), Chung and Ting (1996), Deng and Meguid (1998), Lu et al. (1998, 1999, 2000), Ru (2000a,b), among others. Although the interface crack problem (Kuo and Barnett, 1991; Suo et al., 1992) and interface inclusion problem (Deng and Meguid, 1998) in piezoelectric bimaterials have been addressed and solved, the mixed boundary value problems at piezoelectric bimaterial interface have not yet been studied thoroughly. The mixed boundary value problem discussed in the present work can be interpreted as that a conducting rigid line inclusion is embedded at the interface of dissimilar piezoelectric half planes, and is debonded due to external thermal–mechanical–electrical loading, so that an insulating crack is formed on one side of the line inclusion. First, the standard Stroh formalism (8-D) as well as its modifications is presented, and degenerate cases in which two or more Stroh eigenvalues and their associated Stroh eigenvectors become equal are also considered, then we consider the special mixed boundary value problem in which a debonded conducting rigid line inclusion is embedded at the interface of two piezoelectric half planes and we employ the standard Stroh formalism to obtain an exact solution to the problem. During the solving process, an explicit solution for stress singularities is obtained and this explicit solution can be considered as a proper supplement to Ting's solution (Ting, 1986). The modified Stroh formalism can be applied to treat other more general mixed boundary value problems, e.g., a conducting crack is formed on one side of an interface insulating rigid inclusion. Finally we find that various forms of interface defects can be treated in a unified way and existing models for interface defects can be taken as special cases discussed in the present paper. Particularly, the analysis of interface cracks between the embedded electrode layer and piezoelectric ceramics can also be carried out within the unified framework.

2. Standard Stroh formalism and its modifications

Basic equations for linear piezoelectric materials are as follows:

$$\begin{aligned} &\sigma_{ij,j} = 0 \quad D_{i,i} = 0 \\ &\gamma_{ij} = \tfrac{1}{2}(u_{i,j} + u_{j,i}) \quad E_i = -\phi_{,i} \\ &\sigma_{ij} = C_{ijkl}\gamma_{kl} - e_{kij}E_k \quad D_k = e_{kij}\gamma_{ij} + \varepsilon_{kl}E_l \end{aligned} \tag{1}$$

where u_k, ϕ, σ_{ij}, D_i are respectively mechanical displacements, electric potential, stresses and electric displacements; γ_{ij} and E_i are strain tensor and electric field vector; C_{ijkl}, e_{ijk}, ε_{ij} are respectively elastic moduli measured in a constant electric field, piezoelectric constants and dielectric constants measured at constant strain.

For the two-dimensional problem in which the physical quantities only depend on the fixed Cartesian coordinates x and y, the general solution to the above system of partial differential equations is (Suo et al., 1992; Chung and Ting, 1996; Deng and Meguid, 1998; Lu et al., 2000)

$$\begin{aligned}\mathbf{U} &= [\,u_1 \quad u_2 \quad u_3 \quad \phi\,]^T = \mathbf{A}\mathbf{f}(z) + \overline{\mathbf{A}\mathbf{f}(z)} \\ \mathbf{\Phi} &= [\,\Phi_1 \quad \Phi_2 \quad \Phi_3 \quad \Phi_4\,]^T = \mathbf{B}\mathbf{f}(z) + \overline{\mathbf{B}\mathbf{f}(z)}\end{aligned} \tag{2}$$

where the generalized stress function vector $\mathbf{\Phi}$ satisfies the following relationship

$$\begin{aligned}&\sigma_{i1} = -\Phi_{i,2} \quad \sigma_{i2} = \Phi_{i,1} \quad (i = 1\text{–}3) \\ &D_1 = -\Phi_{4,2} \quad D_2 = \Phi_{4,1}\end{aligned} \tag{3}$$

$\mathbf{A}$ and $\mathbf{B}$ are two 4×4 complex matrices defined as

$$\mathbf{A} = [\,\mathbf{a}_1 \quad \mathbf{a}_2 \quad \mathbf{a}_3 \quad \mathbf{a}_4\,] \qquad \mathbf{B} = [\,\mathbf{b}_1 \quad \mathbf{b}_2 \quad \mathbf{b}_3 \quad \mathbf{b}_4\,] \tag{4}$$

$\mathbf{f}(z)$ can be expressed as

$$\mathbf{f}(z) = [\,f_1(z_1) \quad f_2(z_2) \quad f_3(z_3) \quad f_4(z_4)\,]^T \tag{5a}$$

$$z_\alpha = x + p_\alpha y \quad (\alpha = 1\text{–}4) \;\; \mathrm{Im}(p) > 0 \tag{5b}$$

$\mathbf{a}$, $\mathbf{b}$ and p satisfy the following eigenvalue problem

$$\mathbf{N}\begin{bmatrix}\mathbf{a} \\ \mathbf{b}\end{bmatrix} = p\begin{bmatrix}\mathbf{a} \\ \mathbf{b}\end{bmatrix} \tag{6}$$

with

$$\mathbf{N} = \begin{bmatrix}\mathbf{N}_1 & \mathbf{N}_2 \\ \mathbf{N}_3 & \mathbf{N}_1^T\end{bmatrix} \tag{7}$$

$$\mathbf{N}_1 = -\mathbf{T}^{-1}\mathbf{R}^T \tag{8}$$

$$\mathbf{N}_2 = \mathbf{T}^{-1} = \mathbf{N}_2^T \tag{9}$$

$$\mathbf{N}_3 = \mathbf{R}\mathbf{T}^{-1}\mathbf{R}^T - \mathbf{Q} = \mathbf{N}_3^T \tag{10}$$

$$\mathbf{Q} = \begin{bmatrix}\mathbf{Q}^e & \mathbf{e}_{11} \\ \mathbf{e}_{11}^T & -\varepsilon_{11}\end{bmatrix} \quad \mathbf{R} = \begin{bmatrix}\mathbf{R}^e & \mathbf{e}_{21} \\ \mathbf{e}_{12}^T & -\varepsilon_{12}\end{bmatrix} \quad \mathbf{T} = \begin{bmatrix}\mathbf{T}^e & \mathbf{e}_{22} \\ \mathbf{e}_{22}^T & -\varepsilon_{22}\end{bmatrix} \tag{11}$$

and

$$\begin{aligned}&(\mathbf{Q}^e)_{ik} = C_{i1k1} \quad (\mathbf{R}^e)_{ik} = C_{i1k2} \quad (\mathbf{T}^e)_{ik} = C_{i2k2} \quad (i,k = 1\text{–}3) \\ &\mathbf{e}_{ij} = [\,e_{i1j} \quad e_{i2j} \quad e_{i3j}\,]^T \quad (i,j = 1,2)\end{aligned}$$

Since $\mathbf{A}$ and $\mathbf{B}$ satisfy the following normalized orthogonality relation

$$\begin{bmatrix} \mathbf{B}^T & \mathbf{A}^T \\ \overline{\mathbf{B}}^T & \overline{\mathbf{A}}^T \end{bmatrix} \begin{bmatrix} \mathbf{A} & \overline{\mathbf{A}} \\ \mathbf{B} & \overline{\mathbf{B}} \end{bmatrix} = \mathbf{I} \tag{12}$$

then the following three real 4×4 matrices $\mathbf{S}$, $\mathbf{H}$ and $\mathbf{L}$ can be introduced

$$\mathbf{S} = \mathrm{i}(2\mathbf{A}\mathbf{B}^T - \mathbf{I}), \quad \mathbf{H} = 2\mathrm{i}\mathbf{A}\mathbf{A}^T, \quad \mathbf{L} = -2\mathrm{i}\mathbf{B}\mathbf{B}^T \tag{13}$$

The above three real matrices will be frequently used in the following analyses. $\mathbf{H}$ and $\mathbf{L}$ are both symmetric while $\mathbf{SH}$, $\mathbf{LS}$, $\mathbf{H}^{-1}\mathbf{S}$, $\mathbf{S}\mathbf{L}^{-1}$ are antisymmetric. Moreover, $\mathbf{S}$, $\mathbf{H}$ and $\mathbf{L}$ are not entirely independent and are related by

$$\mathbf{H}\mathbf{L} - \mathbf{S}\mathbf{S} = \mathbf{I} \tag{14}$$

In the above, we have presented the standard Stroh formalism. If one or more corresponding components in $\mathbf{U}$ and $\mathbf{\Phi}$ are exchanged, then the following defined $\widetilde{\mathbf{U}}$ and $\widetilde{\mathbf{\Phi}}$ can be obtained

$$\begin{aligned} \widetilde{\mathbf{U}} &= \widetilde{\mathbf{A}}\mathbf{f}(z) + \overline{\widetilde{\mathbf{A}}}\overline{\mathbf{f}(z)} \\ \widetilde{\mathbf{\Phi}} &= \widetilde{\mathbf{B}}\mathbf{f}(z) + \overline{\widetilde{\mathbf{B}}}\overline{\mathbf{f}(z)} \end{aligned} \tag{15}$$

where

$$\widetilde{\mathbf{U}} = (\mathbf{I}_{4\times4} - \mathbf{Y})\mathbf{U} + \mathbf{Y}\mathbf{\Phi}, \quad \widetilde{\mathbf{\Phi}} = \mathbf{Y}\mathbf{U} + (\mathbf{I}_{4\times4} - \mathbf{Y})\mathbf{\Phi} \tag{16a}$$

$$\widetilde{\mathbf{A}} = (\mathbf{I}_{4\times4} - \mathbf{Y})\mathbf{A} + \mathbf{Y}\mathbf{B}, \quad \widetilde{\mathbf{B}} = \mathbf{Y}\mathbf{A} + (\mathbf{I}_{4\times4} - \mathbf{Y})\mathbf{B} \tag{16b}$$

If only the first component is exchanged, then

$$\mathbf{Y} = \mathbf{Y}_1 = \mathrm{diag}[1 \quad 0 \quad 0 \quad 0] \tag{17a}$$

If only the second component is exchanged, then

$$\mathbf{Y} = \mathbf{Y}_2 = \mathrm{diag}[0 \quad 1 \quad 0 \quad 0] \tag{17b}$$

If only the third component is exchanged, then

$$\mathbf{Y} = \mathbf{Y}_3 = \mathrm{diag}[0 \quad 0 \quad 1 \quad 0] \tag{17c}$$

If only the fourth component is exchanged, then

$$\mathbf{Y} = \mathbf{Y}_4 = \mathrm{diag}[0 \quad 0 \quad 0 \quad 1] \tag{17d}$$

If the ith and jth components in $\mathbf{U}$ are exchanged with the two corresponding components in $\mathbf{\Phi}$, then

$$\mathbf{Y} = \mathbf{Y}_i + \mathbf{Y}_j \quad i \neq j \ (i, j = 1\text{–}4) \tag{17e}$$

If the ith, jth and mth components in $\mathbf{U}$ are exchanged with the three corresponding components in $\mathbf{\Phi}$, then

$$\mathbf{Y} = \mathbf{Y}_i + \mathbf{Y}_j + \mathbf{Y}_m \quad i \neq j \neq m \ (i, j, m = 1\text{–}4) \tag{17f}$$

It can be readily proved that $\widetilde{\mathbf{A}}$ and $\widetilde{\mathbf{B}}$ still satisfy the following normalized orthogonality relationship

$$\begin{bmatrix} \widetilde{\mathbf{B}}^T & \widetilde{\mathbf{A}}^T \\ \overline{\widetilde{\mathbf{B}}}^T & \overline{\widetilde{\mathbf{A}}}^T \end{bmatrix} \begin{bmatrix} \widetilde{\mathbf{A}} & \overline{\widetilde{\mathbf{A}}} \\ \widetilde{\mathbf{B}} & \overline{\widetilde{\mathbf{B}}} \end{bmatrix} = \mathbf{I} \tag{18}$$

then similarly three real matrices $\widetilde{\mathbf{S}}$, $\widetilde{\mathbf{H}}$ and $\widetilde{\mathbf{L}}$ can be introduced as follows:

$$\widetilde{\mathbf{S}} = \mathrm{i}(2\widetilde{\mathbf{A}}\widetilde{\mathbf{B}}^T - \mathbf{I}), \quad \widetilde{\mathbf{H}} = 2\mathrm{i}\widetilde{\mathbf{A}}\widetilde{\mathbf{A}}^T, \quad \widetilde{\mathbf{L}} = -2\mathrm{i}\widetilde{\mathbf{B}}\widetilde{\mathbf{B}}^T \tag{19}$$

$\widetilde{\mathbf{H}}$ and $\widetilde{\mathbf{L}}$ are both symmetric while $\widetilde{\mathbf{S}}\widetilde{\mathbf{H}}$, $\widetilde{\mathbf{L}}\widetilde{\mathbf{S}}$, $\widetilde{\mathbf{H}}^{-1}\widetilde{\mathbf{S}}$, $\widetilde{\mathbf{S}}\widetilde{\mathbf{L}}^{-1}$ are antisymmetric. In addition, $\widetilde{\mathbf{S}}$, $\widetilde{\mathbf{H}}$ and $\widetilde{\mathbf{L}}$ will satisfy the following relationship

$$\widetilde{\mathbf{H}}\widetilde{\mathbf{L}} - \widetilde{\mathbf{S}}\widetilde{\mathbf{S}} = \mathbf{I} \tag{20}$$

The above presented modified Stroh formalism will be useful in solving some special mixed boundary value problems.

The previously obtained standard Stroh formalism and its modifications are based on the assumption that the eigenvalue problem Eq. (6) possesses four independent eigenvectors $\xi_i = \begin{bmatrix} \mathbf{a}_i \\ \mathbf{b}_i \end{bmatrix} (i = 1\text{–}4)$ associated with p_i $(i = 1\text{–}4)$. Similar to the discussions for purely anisotropic elastic material (see, Ting, 2000 and the references cited therein), we will endeavor to present general solution $\mathbf{\Pi} = \begin{bmatrix} \mathbf{U} \\ \mathbf{\Phi} \end{bmatrix}$ for degenerate cases in which the number of the independent eigenvectors of Eq. (6) is less than four according to the following four typical classification

- $p_1 = p_2 \neq p_3 \neq p_4 \quad \xi_1 = \xi_2$

$$\mathbf{\Pi} = 2\mathrm{Re}\left\{ f_1(z_1)\xi_1 + \frac{\mathrm{d}}{\mathrm{d}p_1}[f_2(z_1)\xi_1] + f_3(z_3)\xi_3 + f_4(z_4)\xi_4 \right\} \tag{21}$$

  In this degenerate case, there are only three independent eigenvectors.

- $p_1 = p_2 = p_3 \neq p_4 \quad \xi_1 = \xi_2 = \xi_3$

$$\mathbf{\Pi} = 2\mathrm{Re}\left\{ f_1(z_1)\xi_1 + \frac{\mathrm{d}}{\mathrm{d}p_1}[f_2(z_1)\xi_1] + \frac{\mathrm{d}^2}{\mathrm{d}p_1^2}[f_3(z_1)\xi_1] + f_4(z_4)\xi_4 \right\} \tag{22}$$

  In this degenerate case, there are only two independent eigenvectors.

- $p_1 = p_2,\ p_3 = p_4 \quad \xi_1 = \xi_2,\ \xi_3 = \xi_4$

$$\mathbf{\Pi} = 2\mathrm{Re}\left\{ f_1(z_1)\xi_1 + \frac{\mathrm{d}}{\mathrm{d}p_1}[f_2(z_1)\xi_1] + f_3(z_3)\xi_3 + \frac{\mathrm{d}}{\mathrm{d}p_3}[f_4(z_3)\xi_3] \right\} \tag{23}$$

  In this degenerate case, there are also only two independent eigenvectors.

- $p_1 = p_2 = p_3 = p_4 \quad \xi_1 = \xi_2 = \xi_3 = \xi_4$

$$\mathbf{\Pi} = 2\mathrm{Re}\left\{ f_1(z_1)\xi_1 + \frac{\mathrm{d}}{\mathrm{d}p_1}[f_2(z_1)\xi_1] + \frac{\mathrm{d}^2}{\mathrm{d}p_1^2}[f_3(z_1)\xi_1] + \frac{\mathrm{d}^3}{\mathrm{d}p_1^3}[f_4(z_1)\xi_1] \right\} \tag{24}$$

  In this extraordinary degenerate case, there is only one independent eigenvector.

In the above we have not listed all of the possible degenerate cases as done by Ting (2000) for purely anisotropic materials, but we hasten to add that the form of solution for any other degenerate cases will belong to that for one of the above four cases.

3. Exact solution

As shown in Fig. 1, an anisotropic piezoelectric medium #1, which occupies the upper half plane $z \in S^+$, and another anisotropic piezoelectric medium #2, which occupies the lower half plane $z \in S^-$, form an interface $y = 0$. At the portion $|x| < a$ of the interface, there exists a conducting rigid line inclusion whose upper surface has been fully debonded and there is no traction and free charge on this surface; while the lower surface of the inclusion is still perfectly bonded to the piezoelectric medium #2; at the rest portion of

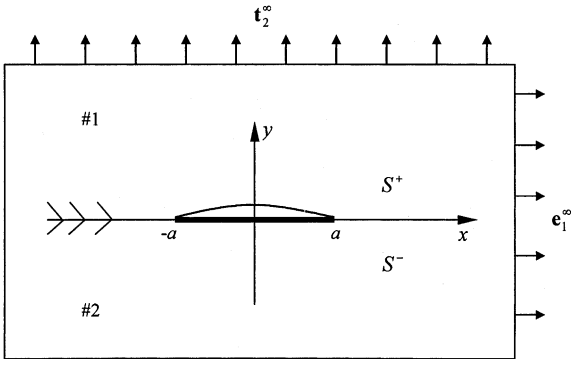

Fig. 1. An interface conducting inclusion debonded at the upper side.

the interface outside the inclusion the two piezoelectric media are still perfectly bonded to each other. The two-phase piezoelectric composite system is subject to remote uniform electromechanical loading $\mathbf{t}_2^\infty = [\,\sigma_{12}^\infty \quad \sigma_{22}^\infty \quad \sigma_{32}^\infty \quad D_2^\infty\,]^T$ and $\mathbf{e}_1^\infty = [\,\gamma_{11}^\infty \quad \gamma_{21}^\infty \quad 2\gamma_{31}^\infty \quad -E_1^\infty\,]^T$.

Based on the superposition principle for a linear system, then it suffices to consider the disturbance fields caused by the debonded conducting rigid line inclusion at the interface. In the disturbance fields, the upper and lower surfaces of the debonded rigid line inclusion should satisfy the following boundary conditions

On the upper side $y = 0^+$, the following is satisfied

$$\mathbf{\Phi}_{1,1} = -\mathbf{t}_2^\infty \quad |x| < a \tag{25}$$

On the other lower side $y = 0^-$, the following is satisfied

$$\mathbf{U}_{2,1} = -\mathbf{e}_1^\infty + \omega[\,0 \quad 1 \quad 0 \quad 0\,]^T \quad |x| < a \tag{26}$$

where in Eq. (26) ω denotes rotation angle of the rigid line about the x_3-axis.

Since the two piezoelectric media are ideally bonded at the rest of the interface outside the line inclusion, then we have

$$\left.\begin{array}{l}\mathbf{\Phi}_1 = \mathbf{\Phi}_2 \\ \mathbf{U}_1 = \mathbf{U}_2\end{array}\right\} \quad |x| > a \tag{27}$$

Define the following two jump potential function vectors $\mathbf{h}_1(z)$ and $\mathbf{h}_2(z)$

$$\mathbf{h}_1(z) = \begin{cases}\mathbf{A}_1\mathbf{f}_1'(z) - \overline{\mathbf{A}}_2\overline{\mathbf{f}}_2'(z) & \mathrm{Im}(z) > 0 \\ \mathbf{A}_2\mathbf{f}_2'(z) - \overline{\mathbf{A}}_1\overline{\mathbf{f}}_1'(z) & \mathrm{Im}(z) < 0\end{cases} \tag{28a}$$

$$\mathbf{h}_2(z) = \begin{cases}\mathbf{B}_1\mathbf{f}_1'(z) - \overline{\mathbf{B}}_2\overline{\mathbf{f}}_2'(z) & \mathrm{Im}(z) > 0 \\ \mathbf{B}_2\mathbf{f}_2'(z) - \overline{\mathbf{B}}_1\overline{\mathbf{f}}_1'(z) & \mathrm{Im}(z) < 0\end{cases} \tag{28b}$$

Noticing the above two defined jump potential function vectors, then the boundary conditions on the interface $y = 0$ can be expressed as

$$\begin{aligned}\mathbf{U}_{1,1} - \mathbf{U}_{2,1} &= \mathbf{h}_1^+(x) - \mathbf{h}_1^-(x) \\ \mathbf{\Phi}_{1,1} - \mathbf{\Phi}_{2,1} &= \mathbf{h}_2^+(x) - \mathbf{h}_2^-(x)\end{aligned} \tag{29}$$

where the superscript '+' denotes approaching the interface $y = 0$ from the upper half plane; similarly, the superscript '−' indicates approaching the interface $y = 0$ from the lower half plane.

From the above equation, it can be found that $\mathbf{h}_1(z)$ represents jumps in the tangential derivative with respect to the interface of displacements and electric potential across the interface and when $|z| \to \infty$, $\mathbf{h}_1(z) = \mathbf{0}(z^{-2})$; while $\mathbf{h}_2(z)$ represents jumps in tractions and normal component of electric displacements across the interface and when $|z| \to \infty$, $\mathbf{h}_2(z) = \mathbf{0}(z^{-2})$. The original holomorphic function vectors $\mathbf{f}_1'(z)$, $\mathbf{f}_2'(z)$ and their analytical continuations $\overline{\mathbf{f}}_1'(\mathbf{z})$, $\overline{\mathbf{f}}_2'(z)$ can be expressed in terms of the two newly defined function vectors $\mathbf{h}_1(z)$ and $\mathbf{h}_2(z)$ as follows:

$$\begin{bmatrix} \mathbf{f}_1'(z) \\ \overline{\mathbf{f}}_2'(z) \end{bmatrix} = \begin{bmatrix} \mathrm{i}\mathbf{B}_1^{-1}\mathbf{M}_*^{-1} & \mathbf{B}_1^{-1}\mathbf{M}_1\mathbf{M}^{*-1} \\ -\overline{\mathbf{A}}_2^{-1}\mathbf{M}^{*-1}\mathbf{M}_1 & -\mathrm{i}\overline{\mathbf{A}}_2^{-1}\mathbf{M}^{*-1} \end{bmatrix} \begin{bmatrix} \mathbf{h}_1(z) \\ \mathbf{h}_2(z) \end{bmatrix} \quad \mathrm{Im}(z) > 0 \tag{30a}$$

$$\begin{bmatrix} \overline{\mathbf{f}}_1'(z) \\ \mathbf{f}_2'(z) \end{bmatrix} = \begin{bmatrix} \mathrm{i}\overline{\mathbf{B}}_1^{-1}\overline{\mathbf{M}}_*^{-1} & -\overline{\mathbf{B}}_1^{-1}\overline{\mathbf{M}}_1\overline{\mathbf{M}}^{*-1} \\ \mathbf{A}_2^{-1}\overline{\mathbf{M}}^{*-1}\overline{\mathbf{M}}_1 & -\mathrm{i}\mathbf{A}_2^{-1}\overline{\mathbf{M}}^{*-1} \end{bmatrix} \begin{bmatrix} \mathbf{h}_1(z) \\ \mathbf{h}_2(z) \end{bmatrix} \quad \mathrm{Im}(z) < 0 \tag{30b}$$

where

$$\mathbf{M}_k = -\mathrm{i}\mathbf{B}_k\mathbf{A}_k^{-1} = \mathbf{H}_k^{-1}(\mathbf{I} + \mathrm{i}\mathbf{S}_k) = \mathbf{L}_k(\mathbf{I} - \mathrm{i}\mathbf{S}_k)^{-1} \quad (k = 1, 2) \tag{31a}$$

$$\mathbf{M}^* = \mathbf{M}_1 + \overline{\mathbf{M}}_2 = \mathbf{H}_1^{-1} + \mathbf{H}_2^{-1} + \mathrm{i}(\mathbf{H}_1^{-1}\mathbf{S}_1 - \mathbf{H}_2^{-1}\mathbf{S}_2) \tag{31b}$$

$$\mathbf{M}_* = \mathbf{M}_1^{-1} + \overline{\mathbf{M}}_2^{-1} = \mathbf{L}_1^{-1} + \mathbf{L}_2^{-1} + \mathrm{i}(\mathbf{S}_2\mathbf{L}_2^{-1} - \mathbf{S}_1\mathbf{L}_1^{-1}) \tag{31c}$$

$\mathbf{M}_1$ and $\mathbf{M}_2$ are called the impedance matrices (Suo et al., 1992) and are two Hermitian matrices; $\mathbf{M}^*$ and $\mathbf{M}_*$ are also two Hermitian matrices.

At the ideally bonded portion ($|x| > a$) of the interface, Eq. (27) shall be satisfied and can be expressed as follows:

$$\mathbf{h}^+(x) - \mathbf{h}^-(x) = \mathbf{0} \quad |x| > a \tag{32}$$

where

$$\mathbf{h}(z) = \begin{bmatrix} \mathbf{h}_1(z) \\ \mathbf{h}_2(z) \end{bmatrix} \tag{33}$$

and when $|z| \to \infty$, $\mathbf{h}(z) = \mathbf{0}(z^{-2})$.

On the debonded interface conducting rigid line inclusion ($|x| < a$), Eqs. (25) and (26) shall be satisfied and can be expressed in terms of $\mathbf{h}(z)$ as follows:

$$\mathbf{G}^{-1}\mathbf{h}^+(x) + \overline{\mathbf{G}}^{-1}\mathbf{h}^-(x) = \mathbf{g} \quad |x| < a \tag{34}$$

where in the above equation

$$\mathbf{G}^{-1} = \begin{bmatrix} \mathbf{M}_*^{-1} & -\mathrm{i}\mathbf{M}_1\mathbf{M}^{*-1} \\ \mathrm{i}\mathbf{M}^{*-1}\mathbf{M}_1 & -\mathbf{M}^{*-1} \end{bmatrix} \tag{35a}$$

$$\mathbf{G} = \begin{bmatrix} \mathbf{M}_1^{-1} & -\mathrm{i}\mathbf{I}_{4\times4} \\ \mathrm{i}\mathbf{I}_{4\times4} & -\overline{\mathbf{M}}_2 \end{bmatrix} = \begin{bmatrix} \mathbf{L}_1^{-1} & \mathbf{0} \\ \mathbf{0} & -\mathbf{H}_2^{-1} \end{bmatrix} + \mathrm{i}\begin{bmatrix} -\mathbf{S}_1\mathbf{L}_1^{-1} & -\mathbf{I} \\ \mathbf{I} & \mathbf{H}_2^{-1}\mathbf{S}_2 \end{bmatrix} \tag{35b}$$

$$\mathbf{g} = \mathrm{i}\left\{ \begin{bmatrix} \mathbf{t}_2^\infty \\ \mathbf{e}_1^\infty \end{bmatrix} - \omega\mathbf{q} \right\} \tag{35c}$$

and

$$\mathbf{q} = [\,0 \quad 0 \quad 0 \quad 0 \quad 0 \quad 1 \quad 0 \quad 0\,]^T \tag{35d}$$

From the above two definitions Eqs. (35a) and (35b), it is apparent that $\mathbf{G}$ and $\mathbf{G}^{-1}$ are both 8×8 Hermitian matrices. Eqs. (32) and (34) constitute mutually coupled Riemann–Hilbert problem of vector form (8-D) with discontinuous coefficients. Then the coupled Hilbert problem shall be decoupled through introduction of coordinate transformation. In view of Eq. (34), we consider the following eigenvalue problem

$$(\overline{\mathbf{G}}^{-1} + \mathrm{e}^{2\pi \mathrm{i}\delta}\mathbf{G}^{-1})\mathbf{v} = \mathbf{0} \tag{36}$$

Substituting specific expression for $\mathbf{G}$ (Eqs. (35a)–(35d)) into the above equation and for a non-trivial solution of $\mathbf{v}$, we have

$$\|\mathbf{W} + \mathrm{i}\beta\mathbf{D}\| = 0 \tag{37}$$

where

$$\mathbf{D} = \begin{bmatrix} \mathbf{L}_1^{-1} & \mathbf{0} \\ \mathbf{0} & -\mathbf{H}_2^{-1} \end{bmatrix} \tag{38a}$$

$$\mathbf{W} = \begin{bmatrix} \mathbf{S}_1\mathbf{L}_1^{-1} & \mathbf{I} \\ -\mathbf{I} & -\mathbf{H}_2^{-1}\mathbf{S}_2 \end{bmatrix} \tag{38b}$$

$$\beta = \frac{1 + \mathrm{e}^{2\pi \mathrm{i}\delta}}{1 - \mathrm{e}^{2\pi \mathrm{i}\delta}} \tag{38c}$$

and

$$\mathbf{D} = \mathbf{D}^T, \quad \mathbf{W} = -\mathbf{W}^T \tag{39}$$

Eq. (37) can be further simplified to be

$$\|\mathbf{F} + \mathrm{i}\beta\mathbf{I}\| = 0 \tag{40}$$

where

$$\mathbf{F} = \begin{bmatrix} -\mathbf{S}_1^T & \mathbf{L}_1 \\ \mathbf{H}_2 & \mathbf{S}_2 \end{bmatrix} \tag{41}$$

It can be readily checked that Eq. (40) is equivalent to the following equation

$$\left\| (\mathbf{S}_2\mathbf{S}_1 - \mathbf{H}_2\mathbf{L}_1) + \mathrm{i}\beta(\mathbf{S}_1 + \mathbf{S}_2) + (\mathrm{i}\beta)^2\mathbf{I} \right\| = 0 \tag{42}$$

When the two media are both purely anisotropic elastic materials, the above equation is identical to Ting's result (Ting, 1986). The advantage of adopting Eq. (40) in stead of Eq. (42) will be shown in the following analysis. Noting that $\mathbf{W}$ is real and antisymmetric while $\mathbf{D}$ is real and symmetric, then expanding the determinant Eq. (37) or (40) will result in the following octonary algebraic equation in β

$$\beta^8 - c_6\beta^6 + c_4\beta^4 - c_2\beta^2 + c_0 = 0 \tag{43}$$

where

$$\begin{aligned} c_6 &= -\tfrac{1}{2}\mathrm{tr}(\mathbf{F}^2) = -\tfrac{1}{2}\mathrm{tr}(\mathbf{S}_1^2 + \mathbf{S}_2^2 + 2\mathbf{H}_2\mathbf{L}_1) \\ c_4 &= -\tfrac{1}{8}\left\{ \mathrm{tr}(\mathbf{F}^4) + \|\mathbf{F}\|\mathrm{tr}(\mathbf{F}^{-4}) - \tfrac{1}{2}\left[\mathrm{tr}(\mathbf{F}^2)\right]^2 - \tfrac{1}{2}\|\mathbf{F}\|\left[\mathrm{tr}(\mathbf{F}^{-2})\right]^2 \right\} \\ c_2 &= -\tfrac{1}{2}\|\mathbf{F}\|\mathrm{tr}(\mathbf{F}^{-2}) \\ c_0 &= \|\mathbf{F}\| = \|\mathbf{H}_2\mathbf{L}_1 - \mathbf{S}_2\mathbf{S}_1\| \end{aligned} \tag{44}$$

During the above derivation for c_4, Hamilton–Caylay theorem (Wang and Shi, 1988) has been utilized. Apparently the octonary algebraic equation (43) in β can reduce to a quartic algebraic equation in β^2, and the resulting quartic equation can be solved analytically using standard method to obtain the four roots β^2 and consequently all the eight roots β of Eq. (43). The concrete solution procedure for the quartic equation is still cumbersome and can be found in a common mathematical manual and will not be shown here. It shall be pointed out that although Ting (1986) derived Eq. (42), he only obtained the explicit solution for the case when both the two materials are isotropic; while in the work of Homulka and Keer (1995), the six eigenvalues of the eigenvalue problem also must be obtained numerically. Noting that $c_0 > 0$, then the stress singularities at the tips of the debonded conducting rigid line inclusion can be categorized as follows based on the nature of the eight roots β of Eq. (43).

- *category 1:* Eq. (43) has eight real roots, then

$$\delta_{1,2} = -\tfrac{1}{2} \pm \mathrm{i}\varepsilon_1, \quad \delta_{3,4} = -\tfrac{1}{2} \pm \mathrm{i}\varepsilon_2, \quad \delta_{5,6} = -\tfrac{1}{2} \pm \mathrm{i}\varepsilon_3, \quad \delta_{7,8} = -\tfrac{1}{2} \pm \mathrm{i}\varepsilon_4 \tag{45a}$$

  and the corresponding eight independent eigenvectors of Eq. (36) comprise the following form of modal matrix

$$\mathbf{P} = [\,\mathbf{v}_1 \quad \overline{\mathbf{v}}_1 \quad \mathbf{v}_3 \quad \overline{\mathbf{v}}_3 \quad \mathbf{v}_5 \quad \overline{\mathbf{v}}_5 \quad \mathbf{v}_7 \quad \overline{\mathbf{v}}_7\,] \tag{45b}$$

- *category 2:* Eq. (43) has four real roots and four purely imaginary roots, then

$$\delta_{1,2} = -\tfrac{1}{2} \pm \mathrm{i}\varepsilon_1, \quad \delta_{3,4} = -\tfrac{1}{2} \pm \mathrm{i}\varepsilon_2, \quad \delta_{5,6} = -\tfrac{1}{2} \pm k_1, \quad \delta_{7,8} = -\tfrac{1}{2} \pm k_2 \tag{46a}$$

  and the corresponding eight independent eigenvectors of Eq. (36) comprise the following form of modal matrix

$$\mathbf{P} = [\,\mathbf{v}_1 \quad \overline{\mathbf{v}}_1 \quad \mathbf{v}_3 \quad \overline{\mathbf{v}}_3 \quad \mathbf{v}_5 \quad \mathbf{v}_6 \quad \mathbf{v}_7 \quad \mathbf{v}_8\,] \tag{46b}$$

  In addition, $\mathbf{v}_5$, $\mathbf{v}_6$, $\mathbf{v}_7$, $\mathbf{v}_8$ are real vectors
- *category 3:* Eq. (43) has four real roots and four complex roots, then

$$\delta_{1,2} = -\tfrac{1}{2} \pm \mathrm{i}\varepsilon_1, \quad \delta_{3,4} = -\tfrac{1}{2} \pm \mathrm{i}\varepsilon_2, \quad \delta_{5,6} = -\tfrac{1}{2} \pm \theta_1 + \mathrm{i}\gamma_1, \quad \delta_{7,8} = -\tfrac{1}{2} \pm \theta_1 - \mathrm{i}\gamma_1 \tag{47a}$$

  and the corresponding eight independent eigenvectors of Eq. (36) comprise the following form of modal matrix

$$\mathbf{P} = [\,\mathbf{v}_1 \quad \overline{\mathbf{v}}_1 \quad \mathbf{v}_3 \quad \overline{\mathbf{v}}_3 \quad \mathbf{v}_5 \quad \mathbf{v}_6 \quad \overline{\mathbf{v}}_5 \quad \overline{\mathbf{v}}_6\,] \tag{47b}$$

- *category 4:* Eq. (43) has eight purely imaginary roots, then

$$\delta_{1,2} = -\tfrac{1}{2} \pm k_1, \quad \delta_{3,4} = -\tfrac{1}{2} \pm k_2, \quad \delta_{5,6} = -\tfrac{1}{2} \pm k_3, \quad \delta_{7,8} = -\tfrac{1}{2} \pm k_4 \tag{48a}$$

  and the corresponding eight independent eigenvectors of Eq. (36) comprise the following form of modal matrix

$$\mathbf{P} = [\,\mathbf{v}_1 \quad \mathbf{v}_2 \quad \mathbf{v}_3 \quad \mathbf{v}_4 \quad \mathbf{v}_5 \quad \mathbf{v}_6 \quad \mathbf{v}_7 \quad \mathbf{v}_8\,] \tag{48b}$$

  In addition, $\mathbf{v}_1$, $\mathbf{v}_2$, $\mathbf{v}_3$, $\mathbf{v}_4$, $\mathbf{v}_5$, $\mathbf{v}_6$, $\mathbf{v}_7$, $\mathbf{v}_8$ are all real vectors
- *category 5:* Eq. (43) has four purely imaginary roots and four complex roots, then

$$\delta_{1,2} = -\tfrac{1}{2} \pm k_1, \quad \delta_{3,4} = -\tfrac{1}{2} \pm k_2, \quad \delta_{5,6} = -\tfrac{1}{2} \pm \theta_1 + \mathrm{i}\gamma_1, \quad \delta_{7,8} = -\tfrac{1}{2} \pm \theta_1 - \mathrm{i}\gamma_1 \tag{49a}$$

  and the corresponding eight independent eigenvectors of Eq. (36) comprise the following form of modal matrix

$$\mathbf{P} = [\,\mathbf{v}_1 \quad \mathbf{v}_2 \quad \mathbf{v}_3 \quad \mathbf{v}_4 \quad \mathbf{v}_5 \quad \mathbf{v}_6 \quad \overline{\mathbf{v}}_5 \quad \overline{\mathbf{v}}_6\,] \tag{49b}$$

  In addition, $\mathbf{v}_1$, $\mathbf{v}_2$, $\mathbf{v}_3$, $\mathbf{v}_4$ are real vectors

- *category 6:* Eq. (43) has eight complex roots, then

$$\delta_{1,2} = -\tfrac{1}{2} \pm \theta_1 + \mathrm{i}\gamma_1, \quad \delta_{3,4} = -\tfrac{1}{2} \pm \theta_1 - \mathrm{i}\gamma_1, \quad \delta_{5,6} = -\tfrac{1}{2} \pm \theta_2 + \mathrm{i}\gamma_2, \quad \delta_{7,8} = -\tfrac{1}{2} \pm \theta_2 - \mathrm{i}\gamma_2 \tag{50a}$$

and the corresponding eight independent eigenvectors of Eq. (36) comprise the following form of modal matrix

$$\mathbf{P} = [\,\mathbf{v}_1 \quad \mathbf{v}_2 \quad \overline{\mathbf{v}}_1 \quad \overline{\mathbf{v}}_2 \quad \mathbf{v}_5 \quad \mathbf{v}_6 \quad \overline{\mathbf{v}}_5 \quad \overline{\mathbf{v}}_6\,] \tag{50b}$$

Noticing that ε_i, k_i, θ_i, γ_i appearing in Eqs. (45a)–(50b) are all real quantities and depend on the electroelastic properties of the bimaterials. When the special degenerate case, in which δ is a double root and there exists only one independent eigenvector associated with δ, is encountered, we may have additional stress singularities of the form $r^{\delta}\ln r$ as those encountered in isotropic bimaterials (Ting, 1986; Markenscoff and Ni, 1996).

It should be pointed out here that in the above we list all possible interface stress singularities, some categories for the stress singularities may not exist in real physical world due to certain restrictions on constitutive constants. Noticing $\mathbf{G}^{-1}$ is Hermitian and the above categorization for interface stress singularities, then the following orthogonal relationship with respect to $\mathbf{G}^{-1}$ and $\overline{\mathbf{G}}^{-1}$ can be obtained

$$\mathbf{J}\mathbf{P}^{H}\mathbf{G}^{-1}\mathbf{P} = \mathbf{\Lambda}_1 \quad \mathbf{J}\mathbf{P}^{H}\overline{\mathbf{G}}^{-1}\mathbf{P} = -\mathbf{\Lambda}_1\mathbf{\Lambda} \tag{51}$$

where in the above expression the superscript 'H' means conjugate and transpose of a matrix, $\mathbf{\Lambda}_1$ is a 8×8 diagonal matrix, $\mathbf{\Lambda} = \langle\langle \mathrm{e}^{2\pi\mathrm{i}\delta_\beta}\rangle\rangle$ with β taken from 1 to 8.

For category 1 stress singularities

$$\mathbf{J} = \mathbf{I}_{8\times 8} \tag{52a}$$

For category 2 and 3 stress singularities

$$\mathbf{J} = \begin{bmatrix} \mathbf{I}_{4\times 4} & \mathbf{0}_{4\times 4} \\ \mathbf{0}_{4\times 4} & \mathbf{J}_1 \end{bmatrix} \tag{52b}$$

For categories 4–6 stress singularities

$$\mathbf{J} = \begin{bmatrix} \mathbf{J}_1 & \mathbf{0}_{4\times 4} \\ \mathbf{0}_{4\times 4} & \mathbf{J}_1 \end{bmatrix} \tag{52c}$$

where in Eqs. (52b) and (52c)

$$\mathbf{J}_1 = \begin{bmatrix} 0 & 1 & 0 & 0 \\ 1 & 0 & 0 & 0 \\ 0 & 0 & 0 & 1 \\ 0 & 0 & 1 & 0 \end{bmatrix} \tag{53}$$

Introduce the following transformation

$$\mathbf{h}(z) = \mathbf{P}\hat{\mathbf{h}}(z) \quad \hat{\mathbf{g}} = \mathbf{\Lambda}_1^{-1}\mathbf{J}\mathbf{P}^{H}\mathbf{g} \tag{54}$$

and premultiply Eq. (34) by $\mathbf{J}\mathbf{P}^{H}$, then the following decoupled Riemann–Hilbert problem can be obtained

$$\begin{cases} \hat{\mathbf{h}}^{+}(x) - \mathbf{\Lambda}\hat{\mathbf{h}}^{-}(x) = \hat{\mathbf{g}} & |x| < a \\ \hat{\mathbf{h}}^{+}(x) - \hat{\mathbf{h}}^{-}(x) = \mathbf{0} & |x| > a \end{cases} \tag{55}$$

Here it should be pointed out that since the Hermitian property of $\mathbf{G}^{-1}$ is fully exploited, then inversion of the modal matrix $\mathbf{P}$ can be circumvented during the above decoupling procedure. The decoupling procedure presented here is different from that adopted by Suo et al. (1992), Markenscoff and Ni (1996), Deng and

Meguid (1998) and shall be more elegant and transparent than their approach. In the investigation of Homulka and Keer (1995), they must also utilize inversion of the modal matrix during their solution procedure.

From Eq. (55) and by noticing that when $z \to \infty$ $\hat{\mathbf{h}}(z) = \mathbf{0}(z^{-2})$, then explicit expression for the holomorphic function vector $\hat{\mathbf{h}}(z)$ can be obtained as follows (Muskhelishvili, 1953)

$$\hat{\mathbf{h}}(z) = \left\{\mathbf{I} - \mathbf{X}(z)\langle\langle z + (1+2\delta_\beta)a\rangle\rangle\right\}(\mathbf{I}-\mathbf{\Lambda})^{-1}\mathbf{\Lambda}_1^{-1}\mathbf{J}\mathbf{P}^H\mathbf{g} \tag{56}$$

where

$$\mathbf{X}(z) = \langle\langle (z+a)^{-(1+\delta_\beta)}(z-a)^{\delta_\beta}\rangle\rangle \tag{57}$$

The explicit expression for the holomorphic function vector $\mathbf{h}(z)$ can be obtained from Eqs. (54) and (56) as follows:

$$\mathbf{h}(z) = \mathbf{P}\left\{\mathbf{I} - \mathbf{X}(z)\langle\langle z + (1+2\delta_\beta)a\rangle\rangle\right\}(\mathbf{I}-\mathbf{\Lambda})^{-1}\mathbf{\Lambda}_1^{-1}\mathbf{J}\mathbf{P}^H\mathbf{g} \tag{58}$$

The above obtained holomorphic function vector $\mathbf{h}(z)$ has satisfied equilibrium condition of force and charge on the line inclusion as well as the single-valuedness condition of displacements and electric potential surrounding the crack. In the expressions for $\hat{\mathbf{h}}(z)$ and $\mathbf{h}(z)$, there still contains an unknown real constant ω (rotation angle of the rigid inclusion) and the unknown can be determined by the following condition that the moment of forces acting on the inclusion vanishes.

$$\int_{-a}^{a} x\sigma_{22}^{(2)}(x,0^-)\,\mathrm{d}x = 0 \tag{59}$$

Or can be expressed by $\hat{\mathbf{h}}(z)$ as the following contour integral surrounding the two faces of the line inclusion

$$\mathbf{q}^T\mathbf{P}\oint \hat{\mathbf{h}}(z)z\,\mathrm{d}z = 0 \tag{60}$$

Applying the residue theorem (Zhuang and Zhang, 1984), rotation angle ω of the inclusion about the x_3-axis can be determined to be

$$\omega = \frac{n_1}{n_2} \tag{61}$$

where

$$n_1 = \mathbf{q}^T\mathbf{P}\langle\langle\delta_\beta(1+\delta_\beta)\rangle\rangle(\mathbf{I}-\mathbf{\Lambda})^{-1}\mathbf{\Lambda}_1^{-1}\mathbf{J}\mathbf{P}^H\begin{bmatrix}\mathbf{t}_2^\infty\\ \mathbf{e}_1^\infty\end{bmatrix} \tag{62a}$$

$$n_2 = \mathbf{q}^T\mathbf{P}\langle\langle\delta_\beta(1+\delta_\beta)\rangle\rangle(\mathbf{I}-\mathbf{\Lambda})^{-1}\mathbf{\Lambda}_1^{-1}\mathbf{J}\mathbf{P}^H\mathbf{q} \tag{62b}$$

It can be observed from the above expression for ω that even the two-phase composite system is only subject to remote uniform tension σ_{22}^∞, the line inclusion will in general experience rotation about the x_3-axis due to anisotropic effect of the bimaterials; while for isotropic bimaterials, only remote uniform shear loading σ_{12}^∞ can make the inclusion rotate about the x_3-axis (Markenscoff and Ni, 1996). Up to now, the holomorphic function vector $\mathbf{h}(z)$ has been completely determined. $\mathbf{f}_1'(z)$, $\mathbf{f}_2'(z)$ as well as their analytical continuations $\overline{\mathbf{f}}_1'(z)$, $\overline{\mathbf{f}}_2'(z)$ can be obtained from Eqs. (30a) and (30b) as follows:

$$\begin{bmatrix}\mathbf{f}_1'(z)\\ \overline{\mathbf{f}}_2'(z)\end{bmatrix} = \mathbf{C}\mathbf{G}^{-1}\mathbf{P}\left\{\mathbf{I} - \mathbf{X}(z)\langle\langle z + (1+2\delta_\beta)a\rangle\rangle\right\}(\mathbf{I}-\mathbf{\Lambda})^{-1}\mathbf{\Lambda}_1^{-1}\mathbf{J}\mathbf{P}^H\mathbf{g} \quad \mathrm{Im}(z) > 0 \tag{63a}$$

$$\begin{bmatrix} \overline{\mathbf{f}}_1'(z) \\ \mathbf{f}_2'(z) \end{bmatrix} = -\overline{\mathbf{CG}}^{-1}\mathbf{P}\{\mathbf{I} - \mathbf{X}(z)\langle\langle z + (1+2\delta_\beta)a\rangle\rangle\}(\mathbf{I}-\mathbf{\Lambda})^{-1}\mathbf{\Lambda}_1^{-1}\mathbf{J}\mathbf{P}^H\mathbf{g} \quad \mathrm{Im}(z) < 0 \tag{63b}$$

with

$$\mathbf{C} = \mathrm{i}\begin{bmatrix} \mathbf{B}_1^{-1} & \mathbf{0} \\ \mathbf{0} & \overline{\mathbf{A}}_2^{-1} \end{bmatrix} \tag{64}$$

Employing a translating technique, the explicit full field expressions for $\mathbf{f}_1'(z)$, $\mathbf{f}_2'(z^*)$ and their analytical continuations $\overline{\mathbf{f}}_1'(z)$, $\overline{\mathbf{f}}_2'(\mathbf{z}^*)$ can be obtained as

$$\begin{aligned}\begin{bmatrix} \mathbf{f}_1'(z) \\ \overline{\mathbf{f}}_2'(z^*) \end{bmatrix} &= \mathbf{C}\mathbf{G}^{-1}\mathbf{P}(\mathbf{I}-\mathbf{\Lambda})^{-1}\mathbf{\Lambda}_1^{-1}\mathbf{J}\mathbf{P}^H\mathbf{g} - \sum_{k=1}^{8}\langle\langle z_\beta \mathbf{X}_k(z_\beta)\rangle\rangle\mathbf{C}\mathbf{G}^{-1}\mathbf{P}\mathbf{I}_k(\mathbf{I}-\mathbf{\Lambda})^{-1}\mathbf{\Lambda}_1^{-1}\mathbf{J}\mathbf{P}^H\mathbf{g} \\ &\quad - \sum_{k=1}^{8}\langle\langle \mathbf{X}_k(z_\beta)\rangle\rangle\mathbf{C}\mathbf{G}^{-1}\mathbf{P}\mathbf{I}_k\langle\langle(1+2\delta_\beta)a\rangle\rangle(\mathbf{I}-\mathbf{\Lambda})^{-1}\mathbf{\Lambda}_1^{-1}\mathbf{J}\mathbf{P}^H\mathbf{g} \quad y > 0\end{aligned} \tag{65}$$

$$\begin{aligned}\begin{bmatrix} \overline{\mathbf{f}}_1'(z) \\ \mathbf{f}_2'(z^*) \end{bmatrix} &= -\overline{\mathbf{CG}}^{-1}\mathbf{P}(\mathbf{I}-\mathbf{\Lambda})^{-1}\mathbf{\Lambda}_1^{-1}\mathbf{J}\mathbf{P}^H\mathbf{g} + \sum_{k=1}^{8}\langle\langle z_\beta \mathbf{X}_k(z_\beta)\rangle\rangle\overline{\mathbf{CG}}^{-1}\mathbf{P}\mathbf{I}_k(\mathbf{I}-\mathbf{\Lambda})^{-1}\mathbf{\Lambda}_1^{-1}\mathbf{J}\mathbf{P}^H\mathbf{g} \\ &\quad + \sum_{k=1}^{8}\langle\langle \mathbf{X}_k(z_\beta)\rangle\rangle\overline{\mathbf{CG}}^{-1}\mathbf{P}\mathbf{I}_k\langle\langle(1+2\delta_\beta)a\rangle\rangle(\mathbf{I}-\mathbf{\Lambda})^{-1}\mathbf{\Lambda}_1^{-1}\mathbf{J}\mathbf{P}^H\mathbf{g} \quad y < 0\end{aligned} \tag{66}$$

where in Eqs. (65) and (66)

$$\begin{aligned}&\mathbf{I}_1 = \mathrm{diag}[1\ 0\ 0\ 0\ 0\ 0\ 0\ 0] \quad \mathbf{I}_2 = \mathrm{diag}[0\ 1\ 0\ 0\ 0\ 0\ 0\ 0] \\ &\mathbf{I}_3 = \mathrm{diag}[0\ 0\ 1\ 0\ 0\ 0\ 0\ 0] \quad \mathbf{I}_4 = \mathrm{diag}[0\ 0\ 0\ 1\ 0\ 0\ 0\ 0] \\ &\mathbf{I}_5 = \mathrm{diag}[0\ 0\ 0\ 0\ 1\ 0\ 0\ 0] \quad \mathbf{I}_6 = \mathrm{diag}[0\ 0\ 0\ 0\ 0\ 1\ 0\ 0] \\ &\mathbf{I}_7 = \mathrm{diag}[0\ 0\ 0\ 0\ 0\ 0\ 1\ 0] \quad \mathbf{I}_8 = \mathrm{diag}[0\ 0\ 0\ 0\ 0\ 0\ 0\ 1]\end{aligned} \tag{67}$$

$\mathbf{X}_k(z)$ denotes the kth diagonal component function of $\mathbf{X}(z)$ and the superscript '$*$' is utilized to distinguish the Stroh eigenvalues pertaining to the lower piezoelectric half plane with those pertaining to the upper piezoelectric half plane.

Before ending this section, we point out that as for the mixed boundary value problem in which a conducting crack is formed on one side of an interface insulating rigid line inclusion, the modified Stroh formalism presented in Section 2 with $\mathbf{Y}$ defined by Eq. (17d) should be adopted while the solution procedure carried out in this section keeps unchanged. In solving interface conducting crack and interface insulating inclusion problems, this kind of modified Stroh formalism should better be employed to obtain real form solutions.

4. Expressions for physical quantities

The stress fields, strain fields and electric fields at the ideally bonded part of the interface are distributed as follows:

$$\mathbf{w}_{,1} = 2\mathrm{i}\,\mathrm{Re}\{\mathbf{G}^{-1}\}\mathbf{P}\{\mathbf{I} - \mathbf{X}(x)\langle\langle x + (1+2\delta_\beta)a\rangle\rangle\}(\mathbf{I}-\mathbf{\Lambda})^{-1}\mathbf{\Lambda}_1^{-1}\mathbf{J}\mathbf{P}^H\mathbf{g} \quad |x| > a \tag{68}$$

where

$$\mathbf{w} = \begin{bmatrix} \mathbf{\Phi} \\ \mathbf{U} \end{bmatrix} \tag{69}$$

Notice the physical meaning of $\mathbf{h}(z)$, then the following densities of dislocations and electric potential dislocations $\hat{\mathbf{b}}$ as well as line loads and line charges $\hat{\mathbf{f}}$ are continuously distributed on the line inclusion $|x| < a$

$$\begin{bmatrix} \hat{\mathbf{b}} \\ \hat{\mathbf{f}} \end{bmatrix} = -\mathbf{P}\mathbf{X}^{+}(x)\langle\langle x + (1+2\delta_\beta)a\rangle\rangle(\mathbf{\Lambda}_1\mathbf{\Lambda})^{-1}\mathbf{J}\mathbf{P}^{H}\mathbf{g} \quad |x| < a \tag{70}$$

Integrating the above equation will yield the following closed form expression for jump in generalized displacement vector $\Delta\mathbf{U} = \mathbf{U}_1 - \mathbf{U}_2$ and jump in generalized stress function vector $\Delta\mathbf{\Phi} = \mathbf{\Phi}_1 - \mathbf{\Phi}_2$ on the debonded inclusion $|x| < a$

$$\begin{bmatrix} \Delta\mathbf{U} \\ \Delta\mathbf{\Phi} \end{bmatrix} = (x^2 - a^2)\mathbf{P}\mathbf{X}^{+}(x)(\mathbf{\Lambda}_1\mathbf{\Lambda})^{-1}\mathbf{J}\mathbf{P}^{H}\mathbf{g} \quad |x| < a \tag{71}$$

It is seen from Eq. (68) that stress fields, strain fields and electric fields are all singular at the two tips $x = \pm a$ of the debonded line inclusion. We can categorize the singular distributions of stress fields, strain fields and electric fields as well as the generalized field intensity factor vector $\widetilde{\mathbf{K}}$ as follows:

- category 1 stress singularities

$$\mathbf{w}_{,1}(r) = (2\pi r)^{-1/2}\mathrm{Re}\{\mathbf{G}^{-1}\}\mathrm{Re}\left\{\mathbf{v}_1 r^{\mathrm{i}\varepsilon_1}\widetilde{K}_1 + \mathbf{v}_3 r^{\mathrm{i}\varepsilon_2}\widetilde{K}_3 + \mathbf{v}_5 r^{\mathrm{i}\varepsilon_3}\widetilde{K}_5 + \mathbf{v}_7 r^{\mathrm{i}\varepsilon_4}\widetilde{K}_7\right\} \tag{72a}$$

$$\widetilde{\mathbf{K}} = \begin{bmatrix} \widetilde{K}_1 & \overline{\widetilde{K}}_1 & \widetilde{K}_3 & \overline{\widetilde{K}}_3 & \widetilde{K}_5 & \overline{\widetilde{K}}_5 & \widetilde{K}_7 & \overline{\widetilde{K}}_7 \end{bmatrix}^T \tag{72b}$$

- category 2 stress singularities

$$\mathbf{w}_{,1}(r) = (2\pi r)^{-1/2}\mathrm{Re}\{\mathbf{G}^{-1}\}\left\{\mathrm{Re}\left\{\mathbf{v}_1 r^{\mathrm{i}\varepsilon_1}\widetilde{K}_1 + \mathbf{v}_3 r^{\mathrm{i}\varepsilon_2}\widetilde{K}_3\right\} + \mathbf{v}_5 r^{k_1}\widetilde{K}_5 + \mathbf{v}_6 r^{-k_1}\widetilde{K}_6 + \mathbf{v}_7 r^{k_2}\widetilde{K}_7 + \mathbf{v}_8 r^{-k_2}\widetilde{K}_8\right\} \tag{73a}$$

$$\widetilde{\mathbf{K}} = \begin{bmatrix} \widetilde{K}_1 & \overline{\widetilde{K}}_1 & \widetilde{K}_3 & \overline{\widetilde{K}}_3 & \widetilde{K}_5 & \widetilde{K}_6 & \widetilde{K}_7 & \widetilde{K}_8 \end{bmatrix}^T \tag{73b}$$

  In addition, $\widetilde{K}_5$, $\widetilde{K}_6$, $\widetilde{K}_7$, $\widetilde{K}_8$ are real quantities

- category 3 stress singularities

$$\mathbf{w}_{,1}(r) = (2\pi r)^{-1/2}\mathrm{Re}\{\mathbf{G}^{-1}\}\mathrm{Re}\left\{\mathbf{v}_1 r^{\mathrm{i}\varepsilon_1}\widetilde{K}_1 + \mathbf{v}_3 r^{\mathrm{i}\varepsilon_2}\widetilde{K}_3 + \mathbf{v}_5 r^{\theta_1+\mathrm{i}\gamma_1}\widetilde{K}_5 + \mathbf{v}_6 r^{-\theta_1+\mathrm{i}\gamma_1}\widetilde{K}_6\right\} \tag{74a}$$

$$\widetilde{\mathbf{K}} = \begin{bmatrix} \widetilde{K}_1 & \overline{\widetilde{K}}_1 & \widetilde{K}_3 & \overline{\widetilde{K}}_3 & \widetilde{K}_5 & \widetilde{K}_6 & \overline{\widetilde{K}}_5 & \overline{\widetilde{K}}_6 \end{bmatrix}^T \tag{74b}$$

- category 4 stress singularities

$$\begin{aligned}\mathbf{w}_{,1}(r) = (2\pi r)^{-1/2}\mathrm{Re}\{\mathbf{G}^{-1}\}\Big\{&\mathbf{v}_1 r^{k_1}\widetilde{K}_1 + \mathbf{v}_2 r^{-k_1}\widetilde{K}_2 + \mathbf{v}_3 r^{k_2}\widetilde{K}_3 + \mathbf{v}_4 r^{-k_2}\widetilde{K}_4 + \mathbf{v}_5 r^{k_3}\widetilde{K}_5 + \mathbf{v}_6 r^{-k_3}\widetilde{K}_6 \\ &+ \mathbf{v}_7 r^{k_4}\widetilde{K}_7 + \mathbf{v}_8 r^{-k_4}\widetilde{K}_8\Big\}\end{aligned} \tag{75a}$$

$$\widetilde{\mathbf{K}} = \begin{bmatrix} \widetilde{K}_1 & \widetilde{K}_2 & \widetilde{K}_3 & \widetilde{K}_4 & \widetilde{K}_5 & \widetilde{K}_6 & \widetilde{K}_7 & \widetilde{K}_8 \end{bmatrix}^T \tag{75b}$$

  In addition, $\widetilde{K}_1$, $\widetilde{K}_2$, $\widetilde{K}_3$, $\widetilde{K}_4$, $\widetilde{K}_5$, $\widetilde{K}_6$, $\widetilde{K}_7$, $\widetilde{K}_8$ are all real quantities

- category 5 stress singularities

$$\mathbf{w}_{,1}(r) = (2\pi r)^{-1/2}\mathrm{Re}\{\mathbf{G}^{-1}\}\Big\{\mathbf{v}_1 r^{k_1}\widetilde{K}_1 + \mathbf{v}_2 r^{-k_1}\widetilde{K}_2 + \mathbf{v}_3 r^{k_2}\widetilde{K}_3 + \mathbf{v}_4 r^{-k_2}\widetilde{K}_4 + \mathrm{Re}\Big\{\mathbf{v}_5 r^{\theta_1+\mathrm{i}\gamma_1}\widetilde{K}_5 + \mathbf{v}_6 r^{-\theta_1+\mathrm{i}\gamma_1}\widetilde{K}_6\Big\}\Big\} \tag{76a}$$

$$\widetilde{\mathbf{K}} = \begin{bmatrix}\widetilde{K}_1 & \widetilde{K}_2 & \widetilde{K}_3 & \widetilde{K}_4 & \widetilde{K}_5 & \widetilde{K}_6 & \overline{\widetilde{K}}_5 & \overline{\widetilde{K}}_6\end{bmatrix}^T \tag{76b}$$

In addition, $\widetilde{K}_1$, $\widetilde{K}_2$, $\widetilde{K}_3$, $\widetilde{K}_4$ are real quantities

- category 6 stress singularities

$$\mathbf{w}_{,1}(r) = (2\pi r)^{-1/2}\mathrm{Re}\{\mathbf{G}^{-1}\}\mathrm{Re}\Big\{\mathbf{v}_1 r^{\theta_1+\mathrm{i}\gamma_1}\widetilde{K}_1 + \mathbf{v}_2 r^{-\theta_1+\mathrm{i}\gamma_1}\widetilde{K}_2 + \mathbf{v}_5 r^{\theta_2+\mathrm{i}\gamma_2}\widetilde{K}_5 + \mathbf{v}_6 r^{-\theta_2+\mathrm{i}\gamma_2}\widetilde{K}_6\Big\} \tag{77a}$$

$$\widetilde{\mathbf{K}} = \begin{bmatrix}\widetilde{K}_1 & \widetilde{K}_2 & \overline{\widetilde{K}}_1 & \overline{\widetilde{K}}_2 & \widetilde{K}_5 & \widetilde{K}_6 & \overline{\widetilde{K}}_5 & \overline{\widetilde{K}}_6\end{bmatrix}^T \tag{77b}$$

The above analysis shows that different from the interface crack and interface inclusion (anti-crack) in which four parameters are sufficient to describe the singular fields, eight parameters $\widetilde{\mathbf{K}} = \begin{bmatrix}\widetilde{K}_1 & \widetilde{K}_2 & \widetilde{K}_3 & \widetilde{K}_4 & \widetilde{K}_5 & \widetilde{K}_6 & \widetilde{K}_7 & \widetilde{K}_8\end{bmatrix}^T$ must be employed for a debonded inclusion to describe the singular distribution of stress fields, strain fields and electric fields near the tips of the debonded inclusion.

5. Real form solutions for important physical quantities

The expressions for rotation of the rigid line inclusion (Eqs. (61), (62a) and (62b)), distribution of stress fields, strain fields and electric fields on the interface (Eqs. (68) and (70)), jumps in displacements and electric potential (Eq. (71)) obtained in the previously two sections need the knowledge of modal matrix $\mathbf{P}$, which must be obtained through solving the eigenvalue problem Eq. (36). In this section, we will present real form solutions for these important physical quantities. The modal matrix $\mathbf{P}$ will be absent in the real form solutions and consequently the solving of eigenvalue problem Eq. (36) can be circumvented.

Noticing that the modal matrix $\mathbf{P}$ satisfies the orthogonality relationship Eq. (51), then the following identities can be readily proved

$$\begin{aligned}
&\mathbf{P}\boldsymbol{\Lambda}^0\boldsymbol{\Lambda}_1^{-1}\mathbf{J}\mathbf{P}^H = \mathbf{G} && \mathbf{P}\boldsymbol{\Lambda}^{-1}\boldsymbol{\Lambda}_1^{-1}\mathbf{J}\mathbf{P}^H = -\overline{\mathbf{G}}\\
&\mathbf{P}\boldsymbol{\Lambda}^1\boldsymbol{\Lambda}_1^{-1}\mathbf{J}\mathbf{P}^H = -\mathbf{G}\overline{\mathbf{G}}^{-1}\mathbf{G} && \mathbf{P}\boldsymbol{\Lambda}^{-2}\boldsymbol{\Lambda}_1^{-1}\mathbf{J}\mathbf{P}^H = \overline{\mathbf{G}}\mathbf{G}^{-1}\overline{\mathbf{G}}\\
&\mathbf{P}\boldsymbol{\Lambda}^2\boldsymbol{\Lambda}_1^{-1}\mathbf{J}\mathbf{P}^H = (\mathbf{G}\overline{\mathbf{G}}^{-1})^2\mathbf{G} && \mathbf{P}\boldsymbol{\Lambda}^{-3}\boldsymbol{\Lambda}_1^{-1}\mathbf{J}\mathbf{P}^H = -(\overline{\mathbf{G}}\mathbf{G}^{-1})^2\overline{\mathbf{G}}\\
&\mathbf{P}\boldsymbol{\Lambda}^3\boldsymbol{\Lambda}_1^{-1}\mathbf{J}\mathbf{P}^H = -(\mathbf{G}\overline{\mathbf{G}}^{-1})^3\mathbf{G} && \mathbf{P}\boldsymbol{\Lambda}^{-4}\boldsymbol{\Lambda}_1^{-1}\mathbf{J}\mathbf{P}^H = (\overline{\mathbf{G}}\mathbf{G}^{-1})^3\overline{\mathbf{G}}
\end{aligned} \tag{78}$$

where in the above identities, the terms on the right-hand side only contain matrices $\mathbf{G}$ and $\mathbf{G}^{-1}$ which have been defined by Eqs. (35a) and (35b). On the other hand, if we treat the eight 8×8 diagonal matrices $\boldsymbol{\Lambda}^{-4}$, $\boldsymbol{\Lambda}^{-3}$, $\boldsymbol{\Lambda}^{-2}$, $\boldsymbol{\Lambda}^{-1}$, $\boldsymbol{\Lambda}^0$, $\boldsymbol{\Lambda}^1$, $\boldsymbol{\Lambda}^2$, $\boldsymbol{\Lambda}^3$ as a set of independent bases, then the 8×8 diagonal matrices $\mathbf{I}_m$ $(m = 1, 2, \ldots, 8)$ defined by Eq. (67) can be uniquely expressed in terms of the set of independent bases $\boldsymbol{\Lambda}^{-4}$, $\boldsymbol{\Lambda}^{-3}$, $\boldsymbol{\Lambda}^{-2}$, $\boldsymbol{\Lambda}^{-1}$, $\boldsymbol{\Lambda}^0$, $\boldsymbol{\Lambda}^1$, $\boldsymbol{\Lambda}^2$, $\boldsymbol{\Lambda}^3$ as follows:

$$\mathbf{I}_m = \sum_{n=1}^{8} c_{mn}\boldsymbol{\Lambda}^{(n-5)} \quad (m = 1, 2, \ldots, 8) \tag{79}$$

consequently for any 8×8 diagonal matrix $\mathbf{D}_0 = \langle\langle d_\beta\rangle\rangle$, the following identity can be derived

$$\begin{aligned}\mathbf{P}\mathbf{D}_0\mathbf{\Lambda}_1^{-1}\mathbf{J}\mathbf{P}^H &= \sum_{m=1}^{8} d_m \mathbf{P}\mathbf{I}_m\mathbf{\Lambda}_1^{-1}\mathbf{J}\mathbf{P}^H = \sum_{n=1}^{8}\left(\sum_{m=1}^{8} d_m c_{mn}\right)\mathbf{P}\mathbf{\Lambda}^{(n-5)}\mathbf{\Lambda}_1^{-1}\mathbf{J}\mathbf{P}^H \\ &= \left[e_1(\overline{\mathbf{G}}\mathbf{G}^{-1})^3 - e_2(\overline{\mathbf{G}}\mathbf{G}^{-1})^2 + e_3\overline{\mathbf{G}}\mathbf{G}^{-1} - e_4\mathbf{I}\right]\overline{\mathbf{G}} \\ &\quad + \left[e_5\mathbf{I} - e_6\mathbf{G}\overline{\mathbf{G}}^{-1} + e_7(\mathbf{G}\overline{\mathbf{G}}^{-1})^2 - e_8(\mathbf{G}\overline{\mathbf{G}}^{-1})^3\right]\mathbf{G}\end{aligned} \tag{80}$$

where

$$e_n = \sum_{m=1}^{8} d_m c_{mn} \quad (n = 1, 2, \ldots, 8) \tag{81}$$

The modal matrix $\mathbf{P}$ does not appear in the most right-hand side of identity Eq. (80). Employing Eq. (80), then expressions for rotation of the rigid line inclusion (Eqs. (61), (62a) and (62b)), distribution of stress fields, strain fields and electric fields on the interface (Eqs. (68) and (70)), jumps in displacements and electric potential (Eq. (71)) will also not contain the modal matrix $\mathbf{P}$. Real form solutions for these physical quantities are then obtained.

6. Unification of various interface defects

In this section, we will treat various forms of interface defects within a unified framework. Since the fact that some physical quantities are continuous across these defects, then the component functions in $\mathbf{h}(z)$ associated with these continuous physical quantities will be zero. As a result, $\mathbf{h}(z)$ can be expressed as follows:

$$\mathbf{h}(z) = \mathbf{E}\widetilde{\mathbf{h}}(z) \tag{82}$$

where the real matrix $\mathbf{E}$ will be determined by various specific interface defects and $\widetilde{\mathbf{h}}(z)$ satisfies the following Hilbert problem

$$\begin{cases} \widetilde{\mathbf{G}}^{-1}\widetilde{\mathbf{h}}^+(x) + \overline{\widetilde{\mathbf{G}}}^{-1}\widetilde{\mathbf{h}}^-(x) = \widetilde{\mathbf{g}} & |x| < a \\ \widetilde{\mathbf{h}}^+(x) - \widetilde{\mathbf{h}}^-(x) = 0 & |x| > a \end{cases} \tag{83}$$

where

$$\widetilde{\mathbf{G}}^{-1} = \mathbf{E}^T\mathbf{G}^{-1}E, \quad \widetilde{\mathbf{g}} = \mathbf{E}^T\mathbf{g} \tag{84}$$

Apparently $\widetilde{\mathbf{G}}^{-1}$ is also Hermitian, but its dimension will be lower than that of $\mathbf{G}^{-1}$. In view of Eq. (83), the stress singularities for the interface defect shall satisfy the following eigenvalue problem

$$(\overline{\widetilde{\mathbf{G}}}^{-1} + \mathrm{e}^{2\pi\mathrm{i}\delta}\widetilde{\mathbf{G}}^{-1})\widetilde{\mathbf{v}} = \mathbf{0} \tag{85}$$

In the following we will discuss various possible forms of interface defects. First the following eight vectors are defined

$$\begin{aligned} \mathbf{m}_1 &= [1\ 0\ 0\ 0\ 0\ 0\ 0\ 0]^T & \mathbf{m}_2 &= [0\ 1\ 0\ 0\ 0\ 0\ 0\ 0]^T \\ \mathbf{m}_3 &= [0\ 0\ 1\ 0\ 0\ 0\ 0\ 0]^T & \mathbf{m}_4 &= [0\ 0\ 0\ 1\ 0\ 0\ 0\ 0]^T \\ \mathbf{m}_5 &= [0\ 0\ 0\ 0\ 1\ 0\ 0\ 0]^T & \mathbf{m}_6 &= [0\ 0\ 0\ 0\ 0\ 1\ 0\ 0]^T \\ \mathbf{m}_7 &= [1\ 0\ 0\ 0\ 0\ 0\ 1\ 0]^T & \mathbf{m}_8 &= [0\ 0\ 0\ 0\ 0\ 0\ 0\ 1]^T \end{aligned} \tag{86}$$

- $[-a,a]$ is a conducting inclusion, and the upper debonded side is also conducting

$$\mathbf{E}=[\,\mathbf{m}_1\quad\mathbf{m}_2\quad\mathbf{m}_3\quad\mathbf{m}_5\quad\mathbf{m}_6\quad\mathbf{m}_7\quad\mathbf{m}_8\,] \tag{87}$$

  In this case $\widetilde{\mathbf{G}}^{-1}$ is a 7×7 Hermitian matrix, and there are seven stress singularities, one of which is $-1/2$.
- $[-a,a]$ is an insulating inclusion, and the upper debonded part is also insulating

$$\mathbf{E}=[\,\mathbf{m}_1\quad\mathbf{m}_2\quad\mathbf{m}_3\quad\mathbf{m}_4\quad\mathbf{m}_5\quad\mathbf{m}_6\quad\mathbf{m}_7\,] \tag{88}$$

  In this case $\widetilde{\mathbf{G}}^{-1}$ is a 7×7 Hermitian matrix, and there are seven stress singularities, one of which is $-1/2$.
- $[-a,a]$ is a conducting inclusion, and the upper debonded conducting part is in smooth contact with the inclusion

$$\mathbf{E}=[\,\mathbf{m}_1\quad\mathbf{m}_3\quad\mathbf{m}_5\quad\mathbf{m}_6\quad\mathbf{m}_7\quad\mathbf{m}_8\,] \tag{89}$$

  In this case $\widetilde{\mathbf{G}}^{-1}$ is a 6×6 Hermitian matrix, and there are six stress singularities.
- $[-a,a]$ is an insulating inclusion, and the upper debonded insulating part is in smooth contact with the inclusion

$$\mathbf{E}=[\,\mathbf{m}_1\quad\mathbf{m}_3\quad\mathbf{m}_4\quad\mathbf{m}_5\quad\mathbf{m}_6\quad\mathbf{m}_7\,] \tag{90}$$

  In this case $\widetilde{\mathbf{G}}^{-1}$ is a 6×6 Hermitian matrix, and there are six stress singularities.
- $[-a,a]$ is a traction-free crack, and its upper surface is insulating while its lower surface is conducting

$$\mathbf{E}=[\,\mathbf{m}_1\quad\mathbf{m}_2\quad\mathbf{m}_3\quad\mathbf{m}_4\quad\mathbf{m}_8\,] \tag{91}$$

In this case $\widetilde{\mathbf{G}}^{-1}$ is a 5×5 Hermitian matrix, and there are five stress singularities, one of which is $-1/2$. This model can be applied to analyze an interface crack with its two tips just lodged at the embedded compliant electrode edges. Recently, Ru et al. (1998) have examined interfacial cracking in electrostrictive multilayer systems. Similar issues for piezoelectric multilayer materials remain to be investigated. We notice that most recently, Ru (2000a) studied interface cracks between the embedded electrode layer and piezoelectric ceramic. In his research, the compliant electrode layer is assumed to be embedded at the entire interface. He stated that the resulting non-trivial mixed boundary value problem does not admit a general closed-form solution, and he only obtained an exact elementary solution for a special case in which the two piezoelectric half-planes are poled in opposite directions perpendicular to the electrode layer. Contrary to his statement, we can still obtain a general closed-form solution for this mixed boundary value problem. We can write the resulting 5×5 Hermitian matrix $\widetilde{\mathbf{G}}^{-1}$ defined by Eq. (91) and the 5×1 jump function vector $\widetilde{\mathbf{h}}(z)$ into the following partitioned form

$$\widetilde{\mathbf{G}}^{-1}=\begin{bmatrix}\mathbf{Y}_{11} & \mathbf{Y}_{12}\\ \mathbf{Y}_{12}^{H} & Y_{22}\end{bmatrix}\quad \widetilde{\mathbf{h}}(z)=\begin{bmatrix}\mathbf{\Omega}(z)\\ g(z)\end{bmatrix} \tag{92}$$

where $\mathbf{Y}_{11}$ is a 4×4 Hermitian matrix, $\mathbf{Y}_{12}$ is a 4×1 vector, Y_{22} is a real quantity scalar, $\mathbf{\Omega}(z)$ is a 4×1 function vector. Then the boundary conditions on the interface crack can be expressed as follows

$$\begin{bmatrix}\mathbf{Y}_{11} & \mathbf{Y}_{12}\\ \mathbf{Y}_{12}^{H} & Y_{22}\end{bmatrix}\begin{bmatrix}\mathbf{\Omega}^{+}(x)\\ g^{+}(x)\end{bmatrix}+\begin{bmatrix}\overline{\mathbf{Y}_{11}} & \overline{\mathbf{Y}_{12}}\\ \overline{\mathbf{Y}_{12}^{H}} & Y_{22}\end{bmatrix}\begin{bmatrix}\mathbf{\Omega}^{-}(x)\\ g^{-}(x)\end{bmatrix}=\mathrm{i}\begin{bmatrix}\mathbf{t}_2^{\infty}\\ 0\end{bmatrix}\quad |x|<a \tag{93}$$

Here the last row in the above equation expresses the conditions $E_1^{(2)}=0$ on the defect. Due to the fact that $E_1^{(2)}=0$ establishes along the lower side of the entire real axis, then it follows from Eq. (93) that

$$g(z)=\begin{cases}-\frac{\mathbf{Y}_{12}^{H}}{Y_{22}}\mathbf{\Omega}(z) & \mathrm{Im}(z)>0\\ -\frac{\mathbf{Y}_{12}^{T}}{Y_{22}}\mathbf{\Omega}(z) & \mathrm{Im}(z)<0\end{cases} \tag{94}$$

A substitution of Eq. (94) into Eq. (93) will result in a standard Hilbert condition for $\mathbf{\Omega}(z)$ on the interval $|x|<a$ as follows:

$$\widetilde{\mathbf{G}}_{*}^{-1}\mathbf{\Omega}^{+}(x)+\overline{\widetilde{\mathbf{G}}_{*}^{-1}}\mathbf{\Omega}^{-}(x)=\mathrm{i}\mathbf{t}_{2}^{\infty}\quad |x|<a \tag{95}$$

here the 4×4 Hermitian matrix $\widetilde{\mathbf{G}}_{*}^{-1}$ is defined by

$$\widetilde{\mathbf{G}}_{*}^{-1}=\mathbf{Y}_{11}-\frac{\mathbf{Y}_{12}\mathbf{Y}_{12}^{H}}{Y_{22}} \tag{96}$$

- $[-a,a]$ is an insulating crack

$$\mathbf{E}=[\,\mathbf{m}_1\quad \mathbf{m}_2\quad \mathbf{m}_3\quad \mathbf{m}_4\,] \tag{97}$$

  In this case $\widetilde{\mathbf{G}}^{-1}=\mathbf{M}_{*}^{-1}$ is a 4×4 Hermitian matrix. There are four stress singularities, and the resulting singularities are identical to the results obtained by Kuo and Barnett (1991), Suo et al. (1992).
- $[-a,a]$ is a conducting crack

$$\mathbf{E}=[\,\mathbf{m}_1\quad \mathbf{m}_2\quad \mathbf{m}_3\quad \mathbf{m}_8\,] \tag{98}$$

  In this case $\widetilde{\mathbf{G}}^{-1}$ is a 4×4 Hermitian matrix, and there are four stress singularities.
- $[-a,a]$ is an ideally bonded conducting inclusion

$$\mathbf{E}=[\,\mathbf{m}_5\quad \mathbf{m}_6\quad \mathbf{m}_7\quad \mathbf{m}_8\,] \tag{99}$$

  In this case $\widetilde{\mathbf{G}}^{-1}=-\mathbf{M}^{*-1}$ is a 4×4 Hermitian matrix. There are four stress singularities, and the resulting singularities are identical to the results obtained by Deng and Meguid (1998).
- $[-a,a]$ is an ideally bonded insulating inclusion

$$\mathbf{E}=[\,\mathbf{m}_4\quad \mathbf{m}_5\quad \mathbf{m}_6\quad \mathbf{m}_7\,] \tag{100}$$

  In this case $\widetilde{\mathbf{G}}^{-1}$ is a 4×4 Hermitian matrix, and there are four stress singularities.
- $[-a,a]$ is a permeable crack

$$\mathbf{E}=[\,\mathbf{m}_1\quad \mathbf{m}_2\quad \mathbf{m}_3\,] \tag{101}$$

  In this case $\widetilde{\mathbf{G}}^{-1}$ is a 3×3 Hermitian matrix, and there are three stress singularities, one of which is $-1/2$.
- $[-a,a]$ is a closed crack with its two surfaces in smooth contact with each other

$$\mathbf{E}=[\,\mathbf{m}_1\quad \mathbf{m}_3\,] \tag{102}$$

  In this case $\widetilde{\mathbf{G}}^{-1}$ is a 2×2 Hermitian matrix, and there are two stress singularities. When the in-plane deformations and out-of-plane deformations are decoupled, then $\widetilde{\mathbf{G}}^{-1}$ will be a 2×2 diagonal real matrix and as a result both the two stress singularities will be $-1/2$.
- $[-a,a]$ is a compliant metal electrode layer (Ru, 2000b)

$$\mathbf{E}=\mathbf{m}_8 \tag{103}$$

  In this case $\widetilde{\mathbf{G}}^{-1}$ is the fourth diagonal element of the 4×4 Hermitian matrix $-\mathbf{M}^{*-1}$ and in addition shall be a real scalar, then there is only one stress singularity $-1/2$. In the analysis performed by Ru (2000b), he did not point out explicitly that the singularity should be $-1/2$ for general piezoelectric

bimaterials since (may be) he did not notice the Hermitian property of $\mathbf{M}^{*-1}$. He only pointed out the $-1/2$ singularity in the discussion for two special cases.

We can conceive many other interface boundary condition combinations and they will not be listed here for brevity. If the modified Stroh formalism is employed, then more boundary conditions can be arrived at. In summary, the above analysis demonstrates that stress singularities for various forms of interface defects discussed in this section can be obtained from various condensed matrices $\widetilde{\mathbf{G}}^{-1}$ (or $\widetilde{\mathbf{G}}_{*}^{-1}$) of $\mathbf{G}^{-1}$ (from 7×7 matrix to a real scalar). After the stress singularity δ and its corresponding eigenvector $\widetilde{\mathbf{v}}$ are determined, then the Hilbert problem Eq. (83) can be solved using the methodology presented in Section 3 and consequently analytical solutions for these defects can be obtained.

7. The influence of material orientation

In this section's discussions, we will assume that both the two piezoelectric materials are rotated in counterclock direction by a common angle θ about the x_3-axis. First, we define the following orthogonal transformation matrix $\mathbf{\Omega}$ ($\mathbf{\Omega}\mathbf{\Omega}^T=\mathbf{I}$)

$$\mathbf{\Omega}=\begin{bmatrix}\mathbf{\Psi} & \mathbf{0}\\ \mathbf{0} & \mathbf{\Psi}\end{bmatrix} \tag{104a}$$

$$\mathbf{\Psi}=\begin{bmatrix}\cos\theta & \sin\theta & 0 & 0\\ -\sin\theta & \cos\theta & 0 & 0\\ 0 & 0 & 1 & 0\\ 0 & 0 & 0 & 1\end{bmatrix} \tag{104b}$$

In the new coordinate system the following relationships will hold

$$\mathbf{A}^*=\mathbf{\Psi}\mathbf{A},\quad \mathbf{B}^*=\mathbf{\Psi}\mathbf{B} \tag{105a}$$

$$\mathbf{S}^*=\mathbf{\Psi}\mathbf{S}\mathbf{\Psi}^T,\quad \mathbf{H}^*=\mathbf{\Psi}\mathbf{H}\mathbf{\Psi}^T,\quad \mathbf{L}^*=\mathbf{\Psi}\mathbf{L}\mathbf{\Psi}^T \tag{105b}$$

$$\mathbf{G}^{*-1}=\mathbf{\Omega}\mathbf{G}^{-1}\mathbf{\Omega}^T,\quad \mathbf{G}^*=\mathbf{\Omega}\mathbf{G}\mathbf{\Omega}^T \tag{105c}$$

Observing the eigenvalue problem Eq. (36), it can be readily proved that stress singularity δ will be invariant in the new coordinate system, a conclusion having been similarly drawn for purely anisotropic elastic bimaterials by Ting (1986); while the modal matrix will change in the following way

$$\mathbf{P}^*=\mathbf{\Omega}\mathbf{P} \tag{106}$$

In the new coordinate system, the orthogonal relationship Eq. (51) still holds in view of Eqs. (105c) and (106), while in the new coordinate system the rotation angle ω^* of the line inclusion about the x_3-axis can be expressed as follows:

$$\omega^*=\frac{n_1^*}{n_2^*} \tag{107}$$

where

$$n_1^*=\mathbf{q}^T\mathbf{\Omega}\mathbf{P}\langle\langle\delta_\beta(1+\delta_\beta)\rangle\rangle(\mathbf{I}-\mathbf{\Lambda})^{-1}\mathbf{\Lambda}_1^{-1}\mathbf{J}\mathbf{P}^H\mathbf{\Omega}^T\begin{bmatrix}\mathbf{t}_2^\infty\\ \mathbf{e}_1^\infty\end{bmatrix} \tag{108a}$$

$$n_2^*=\mathbf{q}^T\mathbf{\Omega}\mathbf{P}\langle\langle\delta_\beta(1+\delta_\beta)\rangle\rangle(\mathbf{I}-\mathbf{\Lambda})^{-1}\mathbf{\Lambda}_1^{-1}\mathbf{J}\mathbf{P}^H\mathbf{\Omega}^T\mathbf{q} \tag{108b}$$

In the new coordinate system, the stress fields, strain fields and electric fields on the ideally bonded part of the interface are distributed as follows:

$$\mathbf{w}_{,1}^{*} = 2\mathrm{i}\boldsymbol{\Omega}\mathrm{Re}\left\{\mathbf{G}^{-1}\right\}\mathbf{P}\left\{\mathbf{I}-\mathbf{X}(x)\langle\langle x+(1+2\delta_{\beta})a\rangle\rangle\right\}(\mathbf{I}-\boldsymbol{\Lambda})^{-1}\boldsymbol{\Lambda}_{1}^{-1}\mathbf{J}\mathbf{P}^{H}\boldsymbol{\Omega}^{T}\mathbf{g}^{*} \quad |x|>a \tag{109}$$

where $\mathbf{g}^{*}$ is similarly defined by Eq. (35c) with ω replaced by ω^{*}.

In the new coordinate system, the following densities of dislocations and electric potential dislocations $\hat{\mathbf{b}}^{*}$ as well as line loads and line charges $\hat{\mathbf{f}}^{*}$ are continuously distributed on the line inclusion $|x|<a$

$$\begin{bmatrix}\hat{\mathbf{b}}^{*}\\ \hat{\mathbf{f}}^{*}\end{bmatrix} = -\boldsymbol{\Omega}\mathbf{P}\mathbf{X}^{+}(x)\langle\langle x+(1+2\delta_{\beta})a\rangle\rangle(\boldsymbol{\Lambda}_{1}\boldsymbol{\Lambda})^{-1}\mathbf{J}\mathbf{P}^{H}\boldsymbol{\Omega}^{T}\mathbf{g}^{*} \quad |x|<a \tag{110}$$

In the new coordinate system, closed form expression for jump in generalized displacement vector $\Delta\mathbf{U}^{*}=\mathbf{U}_{1}^{*}-\mathbf{U}_{2}^{*}$ and jump in generalized stress function vector $\Delta\boldsymbol{\Phi}^{*}=\boldsymbol{\Phi}_{1}^{*}-\boldsymbol{\Phi}_{2}^{*}$ on $|x|<a$ can be obtained as

$$\begin{bmatrix}\Delta\mathbf{U}^{*}\\ \Delta\boldsymbol{\Phi}^{*}\end{bmatrix} = (x^{2}-a^{2})\boldsymbol{\Omega}\mathbf{P}\mathbf{X}^{+}(x)(\boldsymbol{\Lambda}_{1}\boldsymbol{\Lambda})^{-1}\mathbf{J}\mathbf{P}^{H}\boldsymbol{\Omega}^{T}\mathbf{g}^{*} \quad |x|<a \tag{111}$$

As for the various interface defects discussed in Section 6, we find that the stress singularities for three cases will change under rotation about the x_3-axis. Namely,

1. $[-a,a]$ is a conducting inclusion, and the upper debonded conducting part is in smooth contact with the line inclusion;
2. $[-a,a]$ is an insulating inclusion, and the upper debonded insulating part is in smooth contact with the line inclusion;
3. $[-a,a]$ is a closed crack with its two surfaces in smooth contact with each other.

The stress singularities for the rest of the cases will be invariant under rotation of coordinate system about the x_3-axis. Apparently, when the two materials are rotated by different angles, the stress singularities for all of the interface defects will change.

8. Results and discussions

In this section several illustrative numerical examples will be presented to portray the theoretical results obtained in the previously several sections. During the calculations, we utilize material combinations of PZT-4, PZT-5H, Zn and SiC, of which the constitutive constants are listed in Table 1. Among the four materials, PZT-4 and PZT-5H are two piezoelectric materials while Zn and SiC (Homulka and Keer, 1995) are two non-piezoelectric materials.

8.1. Interface stress singularities

Table 2 presents stress singularities for the case in which an insulating crack is formed on the upper side of a conducting interface inclusion, $\delta_{1,2}$ are two out-of-plane stress singularities. From the last four rows in the Table, we find that except the two additional electric field singularities $\delta_{3,4}=-0.5\pm0.25$, all the rest six singularities are the same as those obtained by Homulka and Keer (1995) up to the sixth and seventh digit after the point. This verifies from one aspect the correctness of the explicit solution for stress singularities obtained in this paper. We can also find that all the stress singularities will be non-oscillatory real power type for the case when the debonded inclusion is embedded in a homogeneous transversely isotropic

Table 1
The constitutive constants for the four materials

No.	Material	C_{11}	C_{12}	C_{13}	C_{33}	C_{44}
1	PZT-4	140.20	78.92	75.65	115.77	25.25
2	PZT-5H	126.00	55.00	53.00	117.00	35.30
3	Zn	161.00	34.20	50.10	61.00	38.30
4	SiC	479.00	97.80	55.30	521.40	148.40
		e_{31}	e_{33}	e_{15}	ε_{11}	ε_{33}
1	PZT-4	−5.2677	15.4455	12.0000	0.6359	0.5523
2	PZT-5H	−6.5000	23.3000	17.0000	1.5100	1.3000
3	Zn	0	0	0	ε_0	ε_0
4	SiC	0	0	0	ε_0	ε_0

Note: In the above table, unit for elastic constants is GPa; unit for piezoelectric constants is C/m^2; unit for dielectric constants is 10^{-8} C/Vm. $\varepsilon_0 = 8.85 \times 10^{-12}$ C/Vm is the dielectric constant for vacuum and is used as dielectric constant for Zn and SiC.

Table 2
Stress singularities for the case in which an insulating crack is formed on the upper side of an interface conducting inclusion

	$\delta_{1,2}$	$\delta_{3,4}$	$\delta_{5,6}$	$\delta_{7,8}$
1 + 1	-0.5 ± 0.25	-0.5 ± 0.190248	-0.5 ± 0.25	-0.5 ± 0.309752
2 + 2	-0.5 ± 0.25	-0.5 ± 0.230555	-0.5 ± 0.25	-0.5 ± 0.269445
1 + 2	-0.5 ± 0.230857	-0.5 ± 0.147590	$-0.5 \pm 0.258062 + 0.008691$i	$-0.5 \pm 0.258062 - 0.008691$i
2 + 1	-0.5 ± 0.269143	-0.5 ± 0.331843	$-0.5 \pm 0.251649 + 0.023505$i	$-0.5 \pm 0.251649 - 0.023505$i
1 + 3	-0.5 ± 0.205098	-0.5 ± 0.489665	$-0.5 \pm 0.270751 + 0.045913$i	$-0.5 \pm 0.270751 - 0.045913$i
3 + 1	-0.5 ± 0.294902	-0.5 ± 0.009810	$-0.5 \pm 0.249673 + 0.039852$i	$-0.5 \pm 0.249673 - 0.039852$i
1 + 4	-0.5 ± 0.122947	-0.5 ± 0.489666	$-0.5 \pm 0.155135 + 0.106724$i	$-0.5 \pm 0.155135 - 0.106724$i
4 + 1	-0.5 ± 0.377053	-0.5 ± 0.011334	$-0.5 \pm 0.357307 + 0.023255$i	$-0.5 \pm 0.357307 - 0.023255$i
2 + 3	-0.5 ± 0.223799	-0.5 ± 0.492919	$-0.5 \pm 0.277021 + 0.044266$i	$-0.5 \pm 0.277021 - 0.044266$i
3 + 2	-0.5 ± 0.276201	-0.5 ± 0.006692	$-0.5 \pm 0.236710 + 0.052862$i	$-0.5 \pm 0.236710 - 0.052862$i
2 + 4	-0.5 ± 0.136917	-0.5 ± 0.492919	$-0.5 \pm 0.161177 + 0.108041$i	$-0.5 \pm 0.161177 - 0.108041$i
4 + 2	-0.5 ± 0.363083	-0.5 ± 0.007475	$-0.5 \pm 0.347651 + 0.028191$i	$-0.5 \pm 0.347651 - 0.028191$i
3 + 3	-0.5 ± 0.25	-0.5 ± 0.25	$-0.5 \pm 0.25 + 0.04744894844$i	$-0.5 \pm 0.25 - 0.04744894844$i
4 + 4	-0.5 ± 0.25	-0.5 ± 0.25	$-0.5 \pm 0.25 + 0.06621947513$i	$-0.5 \pm 0.25 - 0.06621947513$i
3 + 4	-0.5 ± 0.157924	-0.5 ± 0.25	$-0.5 \pm 0.135268 + 0.09316652305$i	$-0.5 \pm 0.135268 - 0.09316652305$i
4 + 3	-0.5 ± 0.342076	-0.5 ± 0.25	$-0.5 \pm 0.363320 + 0.01046910742$i	$-0.5 \pm 0.363320 - 0.01046910742$i

Note: the number before the sign "+" represents the upper half plane, while the number behind the sign "+" represents the lower half plane.

piezoelectric material, and these singularities belong to Category 4 singularities discussed in Section 3. When the inclusion is embedded in dissimilar media, we find that except that the two out-of-plane singularities and two in-plane singularities are non-oscillatory, all the rest four in-plane singularities will be oscillatory non-square root ones, and this kind of singularities belongs to Category 5 singularities discussed in Section 3.

As a comparison, Table 3 presents stress singularities for the case in which a conducting crack is formed on the upper side of an insulating inclusion. These singularities are obtained by employing the modified Stroh formalism in Section 2. We can find that the two out-of-plane singularities are the same as those in Table 2. We can observe that even when the inclusion is embedded in a homogeneous piezoelectric media, there still exist oscillatory singularities and the eight singularities belong to Category 5 singularities discussed in Section 3. When the inclusion is embedded in dissimilar media, the eight singularities still belong to Category 5 singularities discussed in Section 3. But in this case the degree of oscillation for the four oscillatory singularities will be more serious than that in Table 2.

Table 3
Stress singularities for the case in which a conducting crack is formed on the upper side of an interface insulating inclusion

	$\delta_{1,2}$	$\delta_{3,4}$	$\delta_{5,6}$	$\delta_{7,8}$
$1+1$	-0.5 ± 0.25	-0.5 ± 0.25	$-0.5 \pm 0.25 + 0.112534i$	$-0.5 \pm 0.25 - 0.112534i$
$2+2$	-0.5 ± 0.25	-0.5 ± 0.25	$-0.5 \pm 0.25 + 0.105342i$	$-0.5 \pm 0.25 - 0.105342i$
$1+2$	-0.5 ± 0.230857	-0.5 ± 0.255901	$-0.5 \pm 0.261026 + 0.085685i$	$-0.5 \pm 0.261026 - 0.085685i$
$2+1$	-0.5 ± 0.269143	-0.5 ± 0.253583	$-0.5 \pm 0.231965 + 0.112293i$	$-0.5 \pm 0.231965 - 0.112293i$
$1+3$	-0.5 ± 0.205098	-0.5 ± 0.009274	$-0.5 \pm 0.252177 + 0.055566i$	$-0.5 \pm 0.252177 - 0.055566i$
$3+1$	-0.5 ± 0.294902	-0.5 ± 0.489665	$-0.5 \pm 0.227809 + 0.063143i$	$-0.5 \pm 0.227809 - 0.063143i$
$1+4$	-0.5 ± 0.122947	-0.5 ± 0.007230	$-0.5 \pm 0.122560 + 0.128473i$	$-0.5 \pm 0.122560 - 0.128473i$
$4+1$	-0.5 ± 0.377053	-0.5 ± 0.489671	$-0.5 \pm 0.344777 + 0.029044i$	$-0.5 \pm 0.344777 - 0.029044i$
$2+3$	-0.5 ± 0.223799	-0.5 ± 0.006555	$-0.5 \pm 0.264712 + 0.052050i$	$-0.5 \pm 0.264712 - 0.052050i$
$3+2$	-0.5 ± 0.276201	-0.5 ± 0.492919	$-0.5 \pm 0.220890 + 0.067830i$	$-0.5 \pm 0.220890 - 0.067830i$
$2+4$	-0.5 ± 0.136917	-0.5 ± 0.005821	$-0.5 \pm 0.139435 + 0.123230i$	$-0.5 \pm 0.139435 - 0.123230i$
$4+2$	-0.5 ± 0.363083	-0.5 ± 0.492920	$-0.5 \pm 0.338598 + 0.032175i$	$-0.5 \pm 0.338598 - 0.032175i$

Note: the number before the sign "+" represents the upper half plane, while the number behind the sign "+" represents the lower half plane.

Table 4 lists all the seven singularities for the case in which the upper debonded side of a conducting inclusion is also conducting. The two out-of-plane singularities are still invariant and there exists a common in-plane singularity -0.5, the rest four in-plane singularities are oscillatory non-square root singularities.

In all the above three cases there exist oscillatory singularities and all the singularities are verified numerically to be invariant under rotations about the x_3-axis. The existence of the oscillatory singularities means that the physical quantities such as stresses, strains and electric fields possess oscillatory properties and the physically unacceptable interpenetration of crack surfaces (Ting, 1986). Table 5 presents all the six singularities for the case in which the upper debonded conducting part of the conducting inclusion is in smooth contact with the conducting inclusion. We can find that two out-of-plane singularities still remain unchanged. Except for the case in which the two media are two identical materials, the four in-plane singularities will change under rotations of the coordinate system about the x_3-axis. When the rotation angle is $\theta = 0°$, we find that there are two common in-plane singularities -0.5 and the rest two in-plane singularities are non-oscillatory real power type; when the rotation angle is $\theta = 45°$, we can observe that there still exist oscillatory singularities for $1+4$ combination (PZT-4/SiC) and $2+4$ combination

Table 4
Stress singularities for the case in which a conducting crack is formed on the upper side of an interface conducting inclusion

	$\delta_{1,2}$	δ_3	$\delta_{4,5}$	$\delta_{6,7}$
$1+1$	-0.5 ± 0.25	-0.5	$-0.5 \pm 0.25 + 0.022106i$	$-0.5 \pm 0.25 - 0.022106i$
$2+2$	-0.5 ± 0.25	-0.5	$-0.5 \pm 0.25 + 0.041768i$	$-0.5 \pm 0.25 - 0.041768i$
$1+2$	-0.5 ± 0.230857	-0.5	$-0.5 \pm 0.235001 + 0.034912i$	$-0.5 \pm 0.235001 - 0.034912i$
$2+1$	-0.5 ± 0.269143	-0.5	$-0.5 \pm 0.263648 + 0.029118i$	$-0.5 \pm 0.263648 - 0.029118i$
$1+3$	-0.5 ± 0.205098	-0.5	$-0.5 \pm 0.252159 + 0.055537i$	$-0.5 \pm 0.252159 - 0.055537i$
$3+1$	-0.5 ± 0.294902	-0.5	$-0.5 \pm 0.249670 + 0.03983668i$	$-0.5 \pm 0.249670 - 0.03983668i$
$1+4$	-0.5 ± 0.122947	-0.5	$-0.5 \pm 0.122419 + 0.128441i$	$-0.5 \pm 0.122419 - 0.128441i$
$4+1$	-0.5 ± 0.377053	-0.5	$-0.5 \pm 0.357318 + 0.023245i$	$-0.5 \pm 0.357318 - 0.023245i$
$2+3$	-0.5 ± 0.223799	-0.5	$-0.5 \pm 0.264708 + 0.052041i$	$-0.5 \pm 0.264708 - 0.052041i$
$3+2$	-0.5 ± 0.276201	-0.5	$-0.5 \pm 0.236708 + 0.052855i$	$-0.5 \pm 0.236708 - 0.052855i$
$2+4$	-0.5 ± 0.136917	-0.5	$-0.5 \pm 0.139394 + 0.123212i$	$-0.5 \pm 0.139394 - 0.123212i$
$4+2$	-0.5 ± 0.363083	-0.5	$-0.5 \pm 0.347655 + 0.028187i$	$-0.5 \pm 0.347655 - 0.028187i$

Note: the number before the sign "+" represents the upper half plane, while the number behind the sign "+" represents the lower half plane.

Table 5
Stress singularities for the case in which the upper debonded conducting part of the conducting inclusion is in smooth contact with the conducting inclusion

	$\delta_{1,2}$	$\delta_{3,4}$ (0°)	$\delta_{3,4}$ (45°)	$\delta_{5,6}$ (0°)	$\delta_{5,6}$ (45°)
1 + 1	-0.5 ± 0.25	-0.5	-0.5	-0.5 ± 0.25	-0.5 ± 0.25
2 + 2	-0.5 ± 0.25	-0.5	-0.5	-0.5 ± 0.25	-0.5 ± 0.25
1 + 2	-0.5 ± 0.230857	-0.5	-0.5 ± 0.005869	-0.5 ± 0.234481	-0.5 ± 0.232342
2 + 1	-0.5 ± 0.269143	-0.5	-0.5 ± 0.004467	-0.5 ± 0.263644	-0.5 ± 0.265459
1 + 3	-0.5 ± 0.205098	-0.5	-0.5 ± 0.096964	-0.5 ± 0.254028	-0.5 ± 0.240116
3 + 1	-0.5 ± 0.294902	-0.5	-0.5 ± 0.061871	-0.5 ± 0.288852	-0.5 ± 0.261124
1 + 4	-0.5 ± 0.122947	-0.5	$-0.5 \pm 0.103254 + 0.106630$i	-0.5 ± 0.130965	$-0.5 \pm 0.103254 - 0.106630$i
4 + 1	-0.5 ± 0.377053	-0.5	-0.5 ± 0.055574	-0.5 ± 0.371095	-0.5 ± 0.358564
2 + 3	-0.5 ± 0.223799	-0.5	-0.5 ± 0.070192	-0.5 ± 0.258972	-0.5 ± 0.260357
3 + 2	-0.5 ± 0.276201	-0.5	-0.5 ± 0.054164	-0.5 ± 0.268974	-0.5 ± 0.242948
2 + 4	-0.5 ± 0.136917	-0.5	$-0.5 \pm 0.103600 + 0.088051$i	-0.5 ± 0.139809	$-0.5 \pm 0.103600 - 0.088051$i
4 + 2	-0.5 ± 0.363083	-0.5	-0.5 ± 0.048233	-0.5 ± 0.359847	-0.5 ± 0.348991

Note: the number before the sign "+" represents the upper half plane, while the number behind the sign "+" represents the lower half plane.

(PZT-5H/SiC). In summary, we find that in this model the singularities are rarely oscillatory and the model can be taken as a plausible model for interface defects.

Table 6 presents all the five singularities for the case in which $[-a, a]$ is a traction-free crack whose upper surface is insulating while whose lower surface is conducting. We can find that there exists a common out-of-plane singularity -0.5, among the four in-plane singularities two singularities are oscillatory square root ones and the other two singularities are non-oscillatory real power type.

Table 7 presents all the four singularities for the two cases in which the two surfaces of the crack are simultaneously insulating or conducting. We can find that in both the two cases there exist a common out-of-plane singularity -0.5 and a common in-plane singularity -0.5, for an insulating crack the rest two in-plane singularities can be oscillatory or non-oscillatory; while for a conducting crack all the rest two in-plane singularities are oscillatory square root singularities. Table 8 presents all the four singularities for ideally bonded conducting or insulating rigid line inclusion. We can find that for the two cases there also exist a common out-of-plane singularity -0.5 and a common in-plane singularity -0.5, but contrary to the two crack cases the rest two in-plane singularities for a conducting inclusion may be oscillatory or non-

Table 6
Stress singularities for a crack whose upper surface is insulating while whose lower surface is conducting

	δ_1	$\delta_{2,3}$	$\delta_{4,5}$
1 + 1	-0.5	-0.5	-0.5 ± 0.5
2 + 2	-0.5	-0.5	-0.5 ± 0.5
1 + 2	-0.5	-0.5 ± 0.200481	-0.5 ± 0.018157i
2 + 1	-0.5	-0.5 ± 0.304729	-0.5 ± 0.016444i
1 + 3	-0.5	-0.5 ± 0.490478	-0.5 ± 0.005872i
3 + 1	-0.5	-0.5 ± 0.002223	-0.5 ± 0.108309i
1 + 4	-0.5	-0.5 ± 0.489920	-0.5 ± 0.080988i
4 + 1	-0.5	-0.5 ± 0.000932	-0.5 ± 0.175938i
2 + 3	-0.5	-0.5 ± 0.493348	-0.5 ± 0.004657i
3 + 2	-0.5	-0.5 ± 0.000988	-0.5 ± 0.087779i
2 + 4	-0.5	-0.5 ± 0.493061	-0.5 ± 0.083657i
4 + 2	-0.5	-0.5 ± 0.001939	-0.5 ± 0.154824i

Table 7
Stress singularities for the two cases in which the two surfaces of the crack are simultaneously insulating or conducting

	δ_1	δ_2	$\delta_{3,4}$ (insulating)	$\delta^*_{3,4}$ (conducting)
$1+2$	-0.5	-0.5	-0.5 ± 0.036364	-0.5 ± 0.018622i
$1+3$	-0.5	-0.5	-0.5 ± 0.005188i	-0.5 ± 0.108707i
$1+4$	-0.5	-0.5	-0.5 ± 0.080859i	-0.5 ± 0.176223i
$2+3$	-0.5	-0.5	-0.5 ± 0.004457i	-0.5 ± 0.088023i
$2+4$	-0.5	-0.5	-0.5 ± 0.083623i	-0.5 ± 0.154963i

Table 8
Stress singularities for an ideally bonded conducting or insulating rigid line inclusion

	δ_1	δ_2	$\delta_{3,4}$ (conducting)	$\delta^*_{3,4}$ (insulating)
$1+2$	-0.5	-0.5	-0.5 ± 0.024350i	-0.5 ± 0.054578i
$1+3$	-0.5	-0.5	-0.5 ± 0.119060	-0.5 ± 0.038248i
$1+4$	-0.5	-0.5	-0.5 ± 0.021875	-0.5 ± 0.074543i
$2+3$	-0.5	-0.5	-0.5 ± 0.095665	-0.5 ± 0.048087i
$2+4$	-0.5	-0.5	-0.5 ± 0.009191i	-0.5 ± 0.068080i

oscillatory; while all the rest two in-plane singularities for an insulating inclusion will be oscillatory square root singularities.

Table 9 presents all the three singularities for the case in which a permeable crack lies on $[-a, a]$. We can find that there is a common out-of-plane singularity -0.5 and the rest two in-plane singularities are oscillatory square root singularities. As for the closed crack whose two surfaces are in smooth contact with each other, since in the present discussion the out-of-plane deformations are decoupled from the in-plane deformations, then both the two singularities will be -0.5. The -0.5 singularities are also verified by our numerical calculation.

The present numerical calculations verify that all the stress singularities listed from Tables 6 to 9 will be invariant under rotations about the x_3-axis.

8.2. Rotation of the conducting rigid line inclusion, distribution of tractions on the interface, surface opening displacements and electric potential difference on the debonded inclusion

Since material orientations, combinations of the two materials, external loading conditions, etc will result in an infinite number of possible configurations, here we will only present numerical results for typical configurations. The upper half plane is chosen to be the piezoelectric material PZT-4 while the lower half plane is chosen to be the non-piezoelectric material Zn. To guarantee the contact zones are sufficiently small, the two-phase composite system is subject to remote uniform loading $\mathbf{t}_2^\infty = [\,0 \quad \sigma_{22}^\infty \quad 0 \quad 0\,]^T$, $\mathbf{e}_1^\infty = \mathbf{0}$.

Table 9
Stress singularities for a permeable crack

	δ_1	$\delta_{2,3}$
$1+2$	-0.5	-0.5 ± 0.017156i
$1+3$	-0.5	-0.5 ± 0.005846i
$1+4$	-0.5	-0.5 ± 0.080932i
$2+3$	-0.5	-0.5 ± 0.004649i
$2+4$	-0.5	-0.5 ± 0.083640i

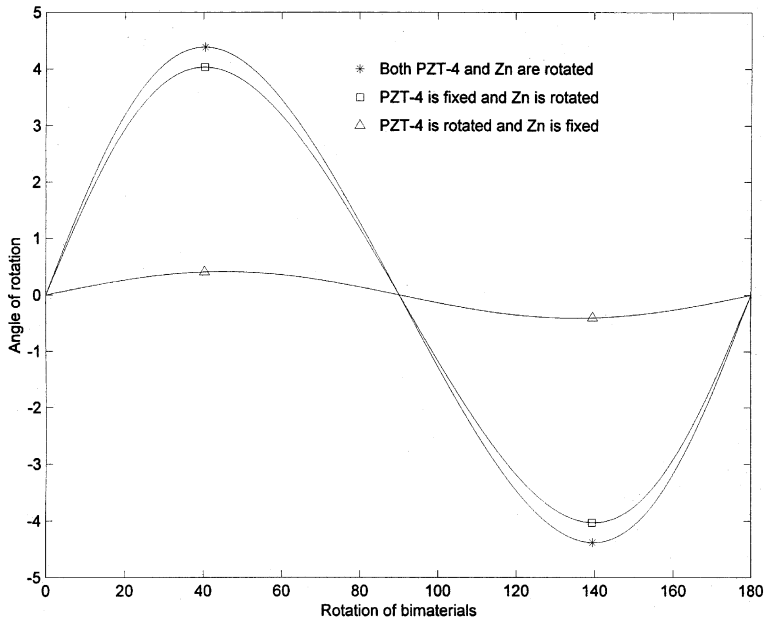

Fig. 2. Variations of normalized rotation angle $\widetilde{\omega} = 10^4\sigma_{22}^{\infty}\omega$ under different rotations of the two materials about the x_3-axis.

When there is no rotation of the coordinate system about the x_3-axis, the rigid line inclusion will also not rotate about the x_3-axis. Fig. 2 depicts the variations of normalized rotation angle $\widetilde{\omega} = 10^4\sigma_{22}^{\infty}\omega$ under different rotations of the two materials about the x_3-axis for three configurations. (a: both the materials are rotated by a common angle; b: the upper PZT-4 is rotated while the lower Zn is fixed; c: the upper PZT-4 is fixed while the lower Zn is rotated). It can be observed from this figure that when both the two materials are rotated by a common angle, the variations of ω are most prominent and the maximum magnitude of rotation angle $\widetilde{\omega}_{\max} = 4.3829$ takes place when $\theta = 40.275°$ and $\theta = 139.725°$; when the upper PZT-4 is rotated while the lower Zn is fixed, the variations of ω are most insignificant with a maximum magnitude of rotation angle $\widetilde{\omega}_{\max} = 0.4095$; when the upper PZT-4 is fixed while the lower Zn is rotated, the variations of ω lie between the above two cases with a maximum magnitude of rotation angle $\widetilde{\omega}_{\max} = 4.0309$. Observing the material constants listed in Table 1, we find that the anisotropic effect of piezoelectric material PZT-4 is weaker than that of the non-piezoelectric material Zn and consequently when only PZT-4 is rotated the variations of ω will be minimal, while when Zn is rotated the variations of ω will be significant.

Figs. 3 and 4 show respectively the normalized shear stress $\sigma_{12}/\sigma_{22}^{\infty}$ and the normalized normal stress $\sigma_{22}/\sigma_{22}^{\infty}$ along the interface $y = 0^-$. Concrete calculations demonstrate that the rotations about the x_3-axis will exert minimal influence on the stress distributions, then only stress distributions for the case in which both the two materials are fixed are shown in the two figures. One can observe from Fig. 3 that except at the regions very near the two tips of the debonded inclusion, the magnitude of shear stress on the rest of the inclusion is very small; while the magnitude of shear stress increases abruptly when approaching the two tips of the inclusion. We can observe from Fig. 4 that tensile stress acting on the lower surface of the inclusion is concentrated in the middle part of the inclusion, while compressive stress is distributed in the regions nears the two tips of the inclusion so as to guarantee balance of force acting on the inclusion in the y direction. The normal stress at the ideally bonded part of the interface $|x| > a$ is always greater than the remote tension σ_{22}^{∞}.

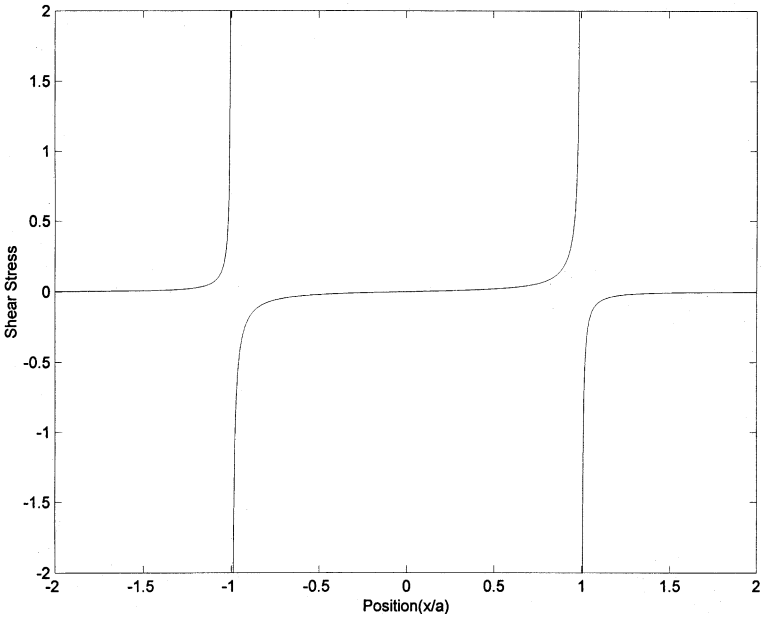

Fig. 3. The normalized shear stress $\sigma_{12}/\sigma_{22}^{\infty}$ along the interface $y = 0^{-}$.

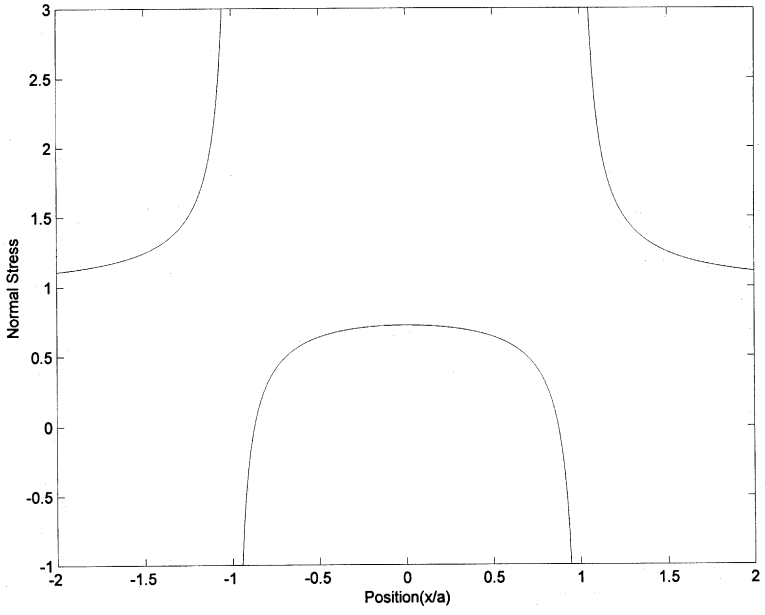

Fig. 4. The normalized normal stress $\sigma_{22}/\sigma_{22}^{\infty}$ along the interface $y = 0^{-}$.

Figs. 5 and 6 show respectively the horizontal opening displacement $\Delta u_1/(a\sigma_{22}^{\infty})$ and vertical opening displacement $\Delta u_2/(a\sigma_{22}^{\infty})$ on the debonded inclusion as well as their variations under different rotations of

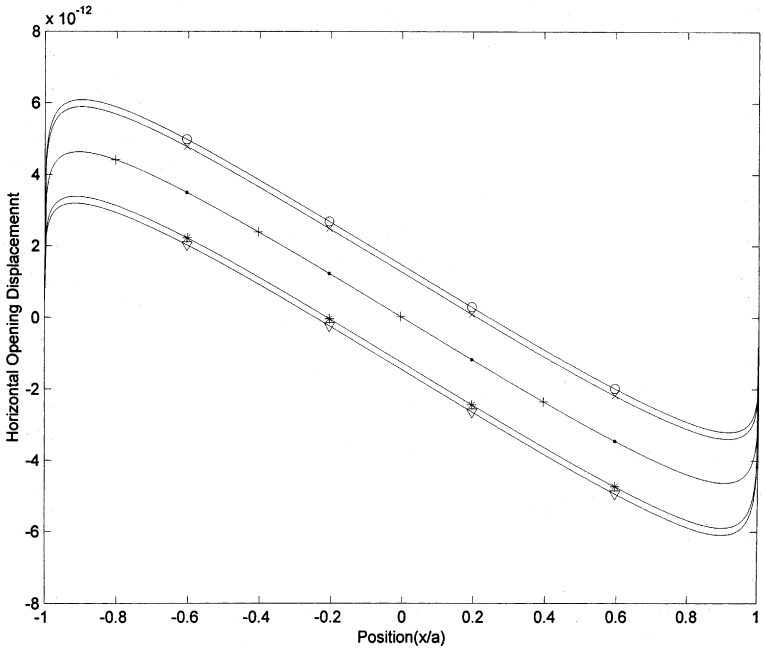

Fig. 5. Horizontal opening displacement $\Delta u_1/(a\sigma_{22}^{\infty})$ on the debonded inclusion and its variations under different rotations about the x_3-axis ((●) −0°; (○) −45°; (×) −60°; (+) −90°; (✳) −120°; (▽) −135°).

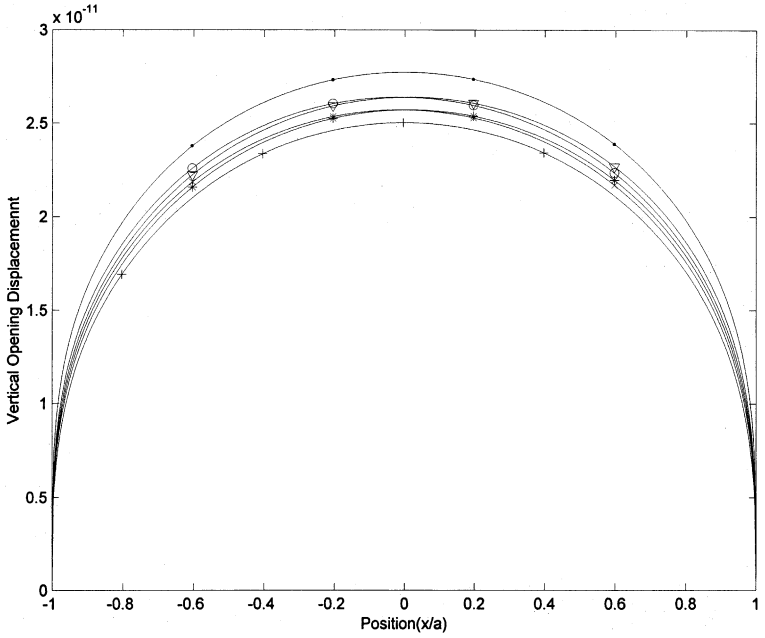

Fig. 6. Vertical opening displacement $\Delta u_2/(a\sigma_{22}^{\infty})$ on the debonded inclusion and its variations under different rotations about the x_3-axis ((●) −0°; (○) −45°; (×) −60°; (+) −90°; (✳) −120°; (▽) −135°).

the coordinate system about the x_3-axis. We can observe from Fig. 5 that the upper debonded part has a tendency to move toward the y-axis. The maximum horizontal opening displacement (6.0874×10^{-12}) occurs when the coordinate system is rotated by 45°; the horizontal opening displacements for the two cases when the coordinate system is rotated by 0° and 90° are identical. A careful checking of the data reveals that $\Delta u_2 < 0$ can occur near the two tips of the debonded inclusion, which is due to the physically unacceptable interpenetration phenomenon of the surfaces caused by the oscillatory stress singularities. Fortunately the interpenetration zones are extremely small (so small that it can not be distinguishable in Fig. 6) and can be ignored under the remote tensile loads. The maximum vertical opening displacement (2.7728×10^{-11}) occurs when the coordinate system is rotated by 0°; the minimum vertical opening displacement (2.5020×10^{-11}) takes place when the coordinate system is rotated by 90°.

Fig. 7 shows the electric potential difference on the debonded inclusion and its variations under different rotations of the coordinate system about the x_3-axis. In comparison with the previously illustrated physical quantities, the material orientation will exert the most prominent influence on the distribution of electric potential difference. We can find that when the rotation angle is increased from 0°, the curves of electric potential difference will be compressed and simultaneously the compressed curves will also rotate in the counterclock direction.

Fig. 8 shows vertical opening displacement $\Delta u_2/(a\sigma_{12}^{\infty})$ on the debonded inclusion under remote shear loads $\mathbf{t}_2^{\infty} = [\,\sigma_{12}^{\infty} \quad 0 \quad 0 \quad 0\,]^T$, $\mathbf{e}_1^{\infty} = \mathbf{0}$. One can observe that under this kind of external loads, $\Delta u_2 < 0$ can occur on the left half part of the inclusion $x \in [-a, 0]$. Adopting the contact zone model may be more reasonable under this kind of loads, but this model will not be further pursued in the present paper.

We have also verified numerically the correctness of the real form solutions presented in Section 5. Since the eigenvalue problem Eq. (36) can be avoided, the accuracy of the real form solution is even better during numerical calculations.

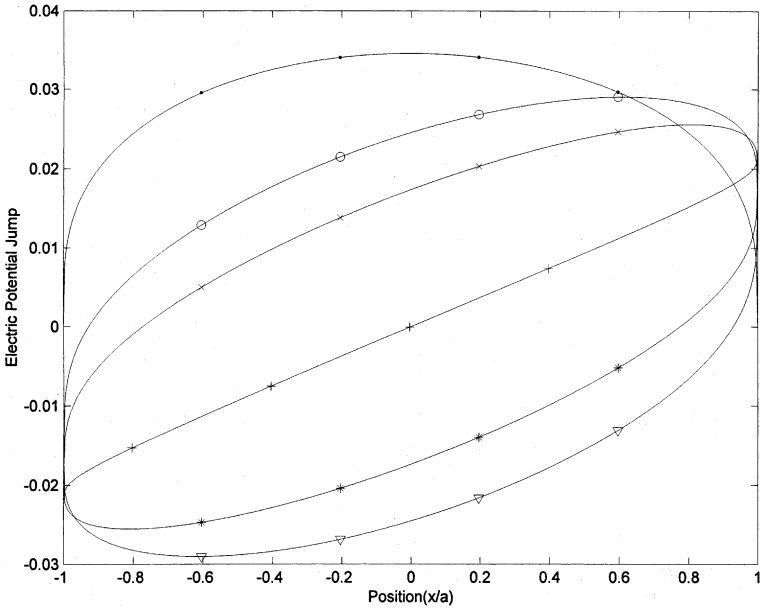

Fig. 7. Electric potential difference on the debonded inclusion and its variations under different rotations about the x_3-axis ((●) −0°; (○) −45°; (×) −60°; (+) −90°; (∗) −120°; (▽) −135°).

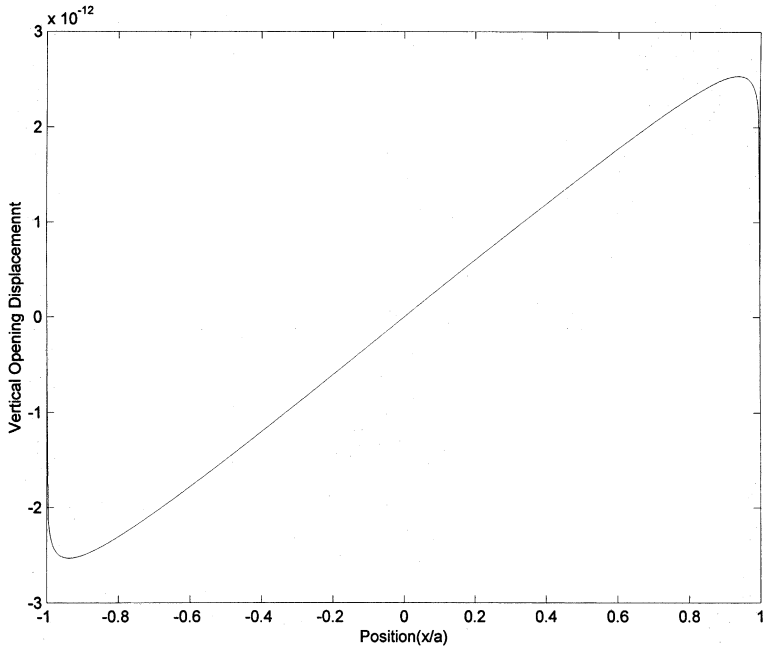

Fig. 8. Vertical opening displacement $\Delta u_2/(a\sigma_{12}^{\infty})$ on the debonded inclusion under remote shear loads $\mathbf{t}_2^{\infty} = \left[\sigma_{12}^{\infty} \quad 0 \quad 0 \quad 0\right]^T$, $\mathbf{e}_1^{\infty} = \mathbf{0}$.

9. Concluding remarks

The standard Stroh formalism is employed to solve a kind of mixed boundary value problems at the interface of dissimilar anisotropic piezoelectric bimaterials. Since the Hermitian property of $\mathbf{G}^{-1}$ is fully exploited, not only the explicit solution for stress singularities can be obtained but also inversion of the modal matrix $\mathbf{P}$ can be circumvented during the decoupling process for the coupled Hilbert problem of vector form. We find that stress singularities for any kind of interface defects can be obtained from $\mathbf{G}^{-1}$, and all of the existing models for interface defects, e.g., insulating crack (Suo et al., 1992), conducting rigid line inclusion (Deng and Meguid, 1998), electrode–ceramic interfacial crack (Ru, 2000a), compliant metal electrode layer (Ru, 2000b), and permeable crack, etc can be treated as special cases discussed in this paper. The numerical results verify the correctness of the theoretical analyses. Meanwhile, the discussions carried out in this paper can be taken as complement to the works of Ting (1986) and Homulka and Keer (1995) when considering electromechanical coupling effects. It is not difficult to apply the methodology presented here to investigate the case when there exist many collinear interface debonded conducting rigid line inclusions and when the composite system is subject to other kinds of thermal–mechanical–electrical loads, e.g., line force and line charge, dislocation and electric-potential dislocation, thermal loads, etc. The success in obtaining the exact solution is due to the powerful tool offered by Stroh formalism.

Acknowledgements

This research was partially supported by the National Natural Science Foundation of China, and partially supported by the Doctorate Foundation of Xi'an Jiaotong University.

References

Chung, M.Y., Ting, T.C.T., 1996. Piezoelectric solid with an elliptic inclusion or hole. Int. J. Solids Struct. 33, 3343–3361.
Clements, D.L., 1971. A crack between dissimilar anisotropic media. Int. J. Eng. Sci. 9, 257–265.
Deng, W., Meguid, S.A., 1998. Analysis of conducting rigid inclusion at the interface of two dissimilar piezoelectric materials. ASME J. Appl. Mech. 62, 76–84.
Gladwell, G.M.L., 1999. On inclusions at a bi-material elastic interface. J. Elasticity 54, 27–41.
Homulka, T.A., Keer, L.M., 1995. A mathematical solution of a special mixed-boundary-value problem of anisotropic elasticity. Q. J. Mech. Appl. Math. 48, 635–658.
Keer, L.M., 1975. Mixed boundary value problems for a penny-shaped cut. J. Elasticity 5, 89–98.
Kuo, C.M., Barnett, D.M., 1991. Stress singularities of interfacial cracks in bonded piezoelectric half-spaces. In: Wu, J.J., Ting, T.C.T., Barnett, D.M. (Eds.), Modern Theory of Anisotropic Elasticity and Applications, Philadelphia: SIAM Proceedings Series, pp. 33–50.
Lu, P., Tan, M.J., Liew, K.M., 1998. Piezothermoelastic analysis of a piezoelectric material with an elliptic cavity under uniform heat flux. Arch. Appl. Mech. 68, 719–733.
Lu, P., Chen, H.B., Tan, M.J., Liew, K.M., 1999. Influence of cavity boundary conditions on the effective electroelastic moduli of piezoelectric ceramic with cavities. Mech. Res. Commun. 26, 229–238.
Lu, P., Tan, M.J., Liew, K.M., 2000. A further investigation of Green's functions for a piezoelectric material with a cavity or a crack. Int. J. Solids Struct. 37, 1065–1078.
Markenscoff, X., Ni, L.Q., 1996. The debonded interface anticrack. ASME J. Appl. Mech. 63, 621–627.
Muskhelishvili, N.I., 1953. Some Basic Problems of the Mathematical Theory of Elasticity. Noordhoff, Groningen.
Ru, C.Q., Mao, X., Epstein, M., 1998. Electric-field induced interfacial cracking in multilayer electrostrictive actuators. J. Mech. Phys. Solids 46, 1301–1308.
Ru, C.Q., 2000a. Electrode-ceramic interfacial cracks in piezoelectric multilayer materials. ASME J. Appl. Mech. 67, 255–261.
Ru, C.Q., 2000b. Exact solution for finite electrode layers embedded at the interface of two piezoelectric half-planes. J. Mech. Phys. Solids 48, 693–708.
Suo, Z., Kuo, C.M., Barnett, D.M., Willis, J.R., 1992. Fracture Mechanics for Piezoelectric Ceramics. J. Mech. Phys. Solids 40, 739–765.
Ting, T.C.T., 1986. Explicit solution and invariance of the singularities at an interface crack in anisotropic composites. Int. J. Solids Struct. 22, 965–983.
Ting, T.C.T., 2000. Recent developments in anisotropic elasticity. Int. J. Solids Struct. 37, 401–409.
Wang, E.F., Shi, S.M., 1988. Advanced Algebra. Beijing University Press, Beijing (in Chinese).
Zhuang, Q.T., Zhang, N.Y., 1984. Complex Variable Function. Beijing University Press, Beijing (in Chinese).